Supporting Information

A Tin Analogue of Propadiene with Cumulated C=Sn Double Bonds

Koh Sugamata,* Teppei Asakawa, and Mao Minoura

Department of Chemistry, College of Science, Rikkyo University
3-34-1, Nishiikebukuro, Toshima-ku, Tokyo 171-8501, Japan

Experimental Procedures

General Procedures

Unless otherwise noted, all experiments were performed under a nitrogen atmosphere. ^{1}H (400 MHz) and ^{13}C NMR (100 MHz) spectra were measured in $CDCl_3$, CD_2Cl_2, C_6D_6, C_7D_8 and, C_4D_8O using JEOL JNM ECS-400SS and ECX-400P spectrometers. The signals arising from residual $CHCl_3$ (7.26 ppm) in $CDCl_3$, $CDCl_2H$ (5.32 ppm) in CD_2Cl_2, CC_6D_5H (7.16 ppm) in C_6D_6, CD_7OH (7.26 ppm) in C_7D_8 and, C_4D_7OH (3.58, 1.72 ppm) in C_4D_8O were used as internal standards for the ^{1}H NMR spectra, and those of $\underline{C}DCl_3$ (77.16 ppm), $\underline{C}D_2Cl_2$ (53.84 ppm) and, $\underline{C}_6D_6$ (128.00 ppm) were used for the ^{13}C NMR spectra. ^{29}Si NMR (79 MHz) spectra were measured in $CDCl_3$, CD_2Cl_2, C_6D_6, and C_4D_8O. ^{119}Sn NMR (148 MHz) spectra were measured in $CDCl_3$, CD_2Cl_2, C_6D_6, and C_4D_8O. Infrared spectrum (IR) was recorded on a JASCO FT/IR-4200 spectrometer. Ultraviolet-visible (UV-vis) spectroscopy was carried out using a JASCO V-603 UV spectrometer. High-resolution mass spectra (HRMS) were recorded using a JEOL JMS-T100LP (ESI) mass spectrometer. All melting points were measured using a SMP-300CT capillary melting point apparatus and are uncorrected.

Synthesis of 2-stannapropadiene ($\mathbf{1_{Sn}}$)

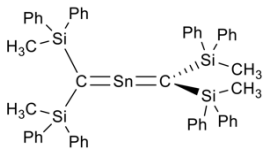

A THF solution (15 mL) of $(MePh_2Si)_2CBr_2$ (1.48 g, 2.61 mmol) at –100 °C was treated dropwise with *t*-BuLi (1.70 M in pentane, 3.07 mL, 5.22 mmol) under vigorous stirring. After 15 min of stirring at this temperature, THF (3 mL) solution of $SnCl_2$ ・dioxane (242 mg, 0.87 mmol) was added dropwise, and the reaction mixture was stirring at this temperature for 2 h. Then the reaction mixture was warmed to room temperature. Subsequently, the reaction mixture was filtrated with benzene to remove inorganic salt. After removal of all volatiles, the residue was washed with hexane to afford 2-stannapropadiene (481 mg, 0.49 mmol, 57%) as a yellow solid.

$\mathbf{1_{Sn}}$: yellow solid, m.p. 174.4-174.6 ºC;

^{1}H NMR (400 MHz, C_6D_6, 298 K) : δ 0.39 (s, 12H), 7.23–7.27 (m, 16H), 7.31–7.35 (m, 6H), 7.42–7.44 (m, 18H); ^{13}C NMR (100 MHz, C_6D_6, 298 K) : δ 141.5, 135.3, 129.7, 128.6, 107.3 (>*C*=Sn), 0.89; ^{29}Si NMR (79 MHz, C_6D_6, 298 K) : δ –17.3; ^{119}Sn NMR (148 MHz, C_6D_6, 298 K) : δ 507; ^{1}H NMR (400 MHz, CD_2Cl_2, 298 K) : δ 0.26 (s, 12H), 7.33–7.35 (m, 16H), 7.39–7.43 (m, 16H), 7.50–7.54 (m, 8H); ^{13}C NMR (100 MHz, CD_2Cl_2, 298 K) : δ 141.4, 135.1, 129.8, 128.4, 106.3 (>*C*=Sn), 0.36; ^{29}Si NMR (79 MHz, CD_2Cl_2, 298 K) : δ –17.9; ^{119}Sn NMR (148 MHz, CD_2Cl_2, 298 K) : δ 496; HRMS (DART) found: *m/z* 933.2256 ($[M+H]^+$). Calcd for $C_{54}H_{52}Si_4Sn$: 933.2301 ($[M+H]^+$). UV-vis (C_6H_6): λ_{max} = 327 nm (ε 7,800 M^{-1} cm^{-1}). UV-vis (THF): λ_{max} = 336 nm (ε 5,600 dm^3 mol^{-1} cm^{-1}), 426 nm (ε 2,000 dm^3 mol^{-1} cm^{-1}). UV-vis (C_6H_6): λ_{max} = 328 nm (ε 6,900 M^{-1} cm^{-1}). IR: ν 930 cm^{-1}, 867 cm^{-1}.

Reaction of $\mathbf{1_{Sn}}$ with H_2O

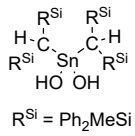

Excess amount of degassed H_2O (3 mL, 0.17 mmol) was added to a benzene solution of $\mathbf{1_{Sn}}$ (100 mg, 0.11 mmol). The reaction mixture was washed with hexane to afford H_2O adduct **2** (73 mg, 0.075 mmol, 68%) as a colorless solid.

2: colorless solid, m.p. 181.2 ºC (dec.);

^{1}H NMR (400 MHz, C_6D_6, 298 K) : δ 0.46 (s, 2H), 0.65 (s, 12H), 0.69 (s, 2H), 7.04–7.06 (m, 8H), 7.21–7.23 (m, 16H), 7.30–7.31 (m, 8H), 7.65–7.67 (m, 8H); ^{13}C NMR (100 MHz, $CDCl_3$, 298 K) : δ 138.3, 137.9, 135.3, 134.6, 129.6, 129.0, 128.1, 127.6, 7.41, –1.04; ^{29}Si NMR (79 MHz, C_6D_6, 298 K) : δ –8.6; ^{119}Sn NMR (148 MHz, C_6D_6, 298 K) : δ 13.2; HRMS (DART) found: *m/z* 969.2513 ([M+H]$^+$). Calcd for $C_{54}H_{56}O_2Si_4Sn$: 969.2467 ([M+H]$^+$).

Reaction of $\mathbf{1_{Sn}}$ with MeLi followed by H_2O

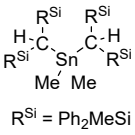

A Et_2O solution of MeLi (0.2 mL, 1.04 M, 0.21 mmol) was added to a THF solution of $\mathbf{1_{Sn}}$ (100 mg, 0.10 mmol) in the presence of 1 drop of 12-crown 4-ether at room temperature. After stirring for 1 h, it was reacted with excess amount of H_2O (1 mL) at the same temperature. After 1h, the reaction mixture was evaporated. The residue was washed with benzene to afford the corresponding protonated compound **3** (41 mg, 0.04 mmol, 38%) as a colorless solid.

3: colorless solid, m.p. 196.3 ºC (dec.) ;

^{1}H NMR (400 MHz, $CDCl_3$, 298 K) : δ –0.28 (s, 6H, J = 26 Hz), 0.49 (s, 12H), 0.75 (s, 2H), 7.01–7.02 (m, 16H), 7.10–7.15 (m, 4H), 7.28–7.36 (m, 20H); ^{13}C NMR (100 MHz, $CDCl_3$, 298 K) : δ139.8, 139.2, 135.0, 134.6, 128.9, 128.4, 127.8, 127.3, 0.26, –0.54, –5.02; ^{29}Si NMR (79 MHz, $CDCl_3$, 298 K) : δ –8.0; ^{119}Sn NMR (148 MHz, $CDCl_3$, 298 K) : δ 24.8; HRMS (DART) found: *m/z* 949.2601 ([M–Me]$^+$). Calcd for $C_{55}H_{57}Si_4Sn$: 949.2569 ([M–Me]$^+$).

Reaction of $\mathbf{1_{Sn}}$ with HCl

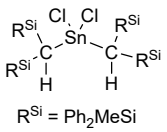

Excess amount of dioxane solution of HCl (0.1 mL, 4 M, 0.43 mmol) was added to a THF solution of $\mathbf{1_{Sn}}$ (100 mg, 0.11 mmol) at –50 ºC. After stirred for 1 h, the reaction mixture was quenched with $NaHCO_3$ and evaporated. The residue was dissolved in benzene and filtrated with celite. The filtrate was evaporated. The residue was washed with MeCN to afford compound **4Cl** (78 mg, 0.08 mmol, 18%) as a colorless solid.

4Cl: colorless solid, m.p. 237.2 ºC (dec.);

^{1}H NMR (400 MHz, $CDCl_3$, 298 K) : δ 0.75 (s, 12H), 1.18 (s, 2H), 6.99–7.00 (m, 16H), 7.12–7.14 (m, 4H), 7.36–7.45 (m, 20H); ^{13}C NMR (100 MHz, $CDCl_3$, 298 K) : δ 138.2, 137.0, 135.4, 134.7, 129.4, 128.8, 128.0, 127.3, 14.6, –1.11; ^{29}Si NMR (79 MHz, $CDCl_3$, 298 K) : δ –9.5; ^{119}Sn NMR (148 MHz, $CDCl_3$, 298 K) : δ 85.0; HRMS (DART) found: *m/z* 1022.1846 ($[M+H_2O]^+$). Calcd for $C_{54}H_{54}Cl_2Si_4Sn$: 1022.1805 ($[M+H_2O]^+$).

Reaction of $\mathbf{1_{Sn}}$ with $SnCl_2$•dioxane

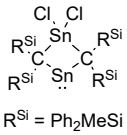

A $SnCl_2$•dioxane (60 mg, 0.22 mmol) was added to a benzene solution of $\mathbf{1_{Sn}}$ (200 mg, 0.22 mmol) at room temperature. After stirred for 1 h, the reaction mixture was evaporated. The residue was washed with hexane to afford the corresponding protonated compound **5Cl** (140 mg, 0.13 mmol, 57%) as a light brown solid.

5Cl: light brown solid, m.p. 138.6 °C (dec.);

^{1}H NMR (400 MHz, C_6D_6, 298 K) : δ 0.66 (s, 12H), 6.93–7.10 (m, 22H), 7.40–7.47 (m, 18H); ^{13}C NMR (100 MHz, C_6D_6, 298 K) : δ 139.0, 138.3, 136.2, 136.1, 129.7, 129.5, 128.6, 128.4, 83.5, 5.73; ^{29}Si NMR (79 MHz, C_6D_6, 298 K) : δ –14.1; ^{119}Sn NMR (148 MHz, C_6D_6, 298 K) : δ 1355, 61; UV-vis (C_6H_6): λ_{max} = 282 nm (ε 7,700 dm^3 mol^{-1} cm^{-1}), 336 nm (ε 2,500 dm^3 mol^{-1} cm^{-1}), 466 nm (ε 1,300 dm^3 mol^{-1} cm^{-1}).

Reaction of $\mathbf{1_{Sn}}$ with $SnBr_2$•dioxane

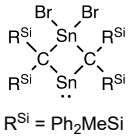

A $SnBr_2$•dioxane (191 mg, 0.69 mmol) was added to a benzene solution of $\mathbf{1_{Sn}}$ (650 mg, 0.69 mmol) at room temperature. After stirred for 1 h, the reaction mixture was evaporated. The residue was washed with hexane to afford the corresponding protonated compound **5Br** (652 mg, 0.54 mmol, 78%) as a light brown solid.

5Br: light brown solid, m.p. 153.4 °C (dec.);
^{1}H NMR (400 MHz, C_6D_6, 298 K) : δ 0.75 (s, 12H), 6.97–7.01 (m, 16H), 7.06–7.10 (m, 8H), 7.38–7.40 (m, 8H), 7.50–7.52 (m, 8H); ^{1}H NMR (400 MHz, toluene-d_8, 298 K) : δ 0.69 (s, 12H), 7.34–7.35 (m, 8H), 7.43–7.45 (m, 8H), The rest of 24H are overlap with toluene-d_8 ; ^{13}C NMR, ^{29}Si NMR and ^{119}Sn NMR could not obtained due to the insolubility.; UV-vis (C_6H_6): λ_{max} = 282 nm (ε 7,900 dm^3 mol^{-1} cm^{-1}), 352 nm (ε 3,300 dm^3 mol^{-1} cm^{-1}), 472 nm (ε 1,300 dm^3 mol^{-1} cm^{-1}).

Reaction of **5Cl** with H_2O

Excess amount of H_2O (1 mL) was added to a benzene solution of **5Cl** (30 mg, 0.027 mmol) and stirring for 1h at room temperature. After that, the reaction mixture was evaporated. The residue was washed with MeCN to afford **4Cl** (5 mg, 0.005 mmol, 18%) as a colorless solid.

Reaction of **5Br** with H_2O

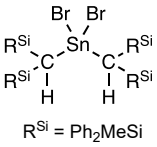

Excess amount of H_2O (1 mL) was added to a benzene solution of **5Br** (60 mg, 0.050 mmol) and stirring for 1h at room temperature. After that, the reaction mixture was evaporated. The residue was washed with MeCN to afford **4Br** (41.5 mg, 0.021 mmol, 42%) as a colorless solid.

4Br: colorless solid, m.p. 237.2 ºC (dec.);
^{1}H NMR (400 MHz, $CDCl_3$, 298 K) : δ 0.83 (s, 12H), 1.50 (s, 2H), 6.97–6.97 (m, 16H), 7.11–7.12 (m, 4H), 7.36–7.39 (m, 20H); ^{13}C NMR (100 MHz, $CDCl_3$, 298 K) : δ 138.3, 137.2, 135.5, 134.7, 129.3, 128.7, 128.0, 127.2, 13.9, –1.0; ^{29}Si NMR (79 MHz, $CDCl_3$, 298 K) : δ –9.1; ^{119}Sn NMR (148 MHz, $CDCl_3$, 298 K) : δ 9.9; HRMS (DART) found: *m/z* 1112.0829 ([M+H_2O]$^+$). Calcd for $C_{54}H_{54}Br_2Si_4Sn$: 1112.0785 ([M+H_2O]$^+$).

Reduction of **5Br** with KC_8

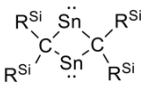

R^{Si} = Ph_2MeSi

A KC_8 (135 mg, 1.00 mmol) was added to a THF of **5Br** (600 mg, 0.50 mmol) at room temperature. After stirred for 3 h, the reaction mixture was filtrated with THF for exclude graphite and the filtrate was evaporated. The residue was washed with benzene to afford **6** (132 mg, 0.13 mmol, 26%) as a purple solid.

6: purple solid, m.p. 187.2 °C (dec.);
^{1}H NMR (400 MHz, C_6D_6, 298 K) : δ 0.47 (s, 12H), 7.07–7.09 (m, 24H), 7.56–7.57 (m, 16H); ^{13}C NMR (100 MHz, C_6D_6, 298 K) : δ 141.9, 134.9, 129.2, 128.7, 3.21, The rest of Sn_2C_2 Carbon could not obtained due to the insolubility.; ^{119}Sn NMR (148 MHz, C_6D_6, 348 K) : δ 2003; ^{1}H NMR (400 MHz, tetrahydrofurane-d_8, 298 K) : δ 0.21 (s, 12H), 7.12–7.16 (m, 16H), 7.21–7.25 (m, 8H), 7.37–7.39 (m, 16H); ^{29}Si NMR (79 MHz, tetrahydrofurane-d_8, 298 K) : δ –25.4; HRMS (DART) found: *m/z* 1067.1207 ([M+OH]$^+$). Calcd for $C_{54}H_{52}Si_4Sn_2$: 1067.1228 ([M+OH]$^+$). UV-vis (THF): λ_{max} = 304 nm (ε 6,700 dm^3 mol^{-1} cm^{-1}), 558 nm (ε 700 dm^3 mol^{-1} cm^{-1}).

Photoreaction of $\mathbf{1_{Sn}}$

C_6D_6 solution of $\mathbf{1_{Sn}}$ (30 mg, 0.03 mmol) in Pyrex J-young tube was irradiated a 100 W high-pressure mercury lamp for 3 days. The reaction mixture was evaporated. The residue was washed with hexane to afford **6** (2 mg, 0.002 mmol, 6%) as a purple solid.

NMR Spectroscopic Analysis

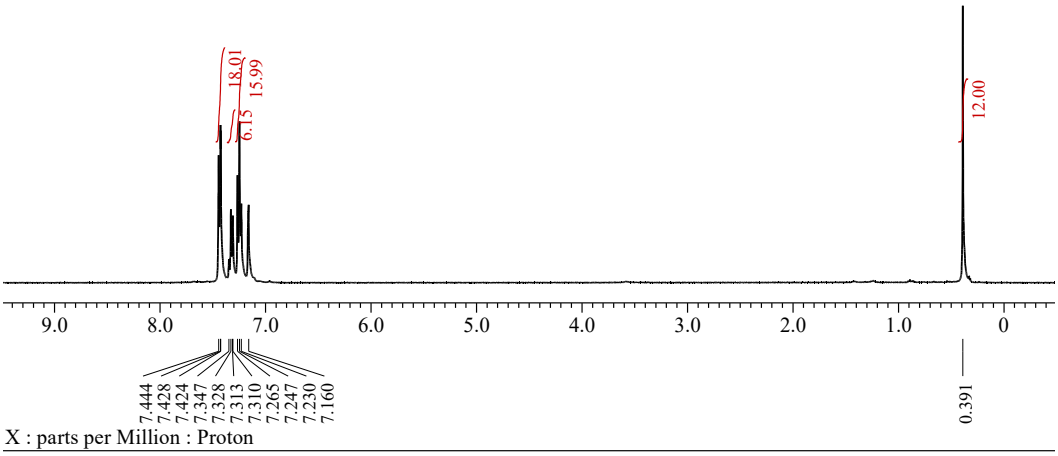

Figure S1. ^{1}H NMR spectrum (C_6D_6, 400 MHz) of $\mathbf{1_{Sn}}$

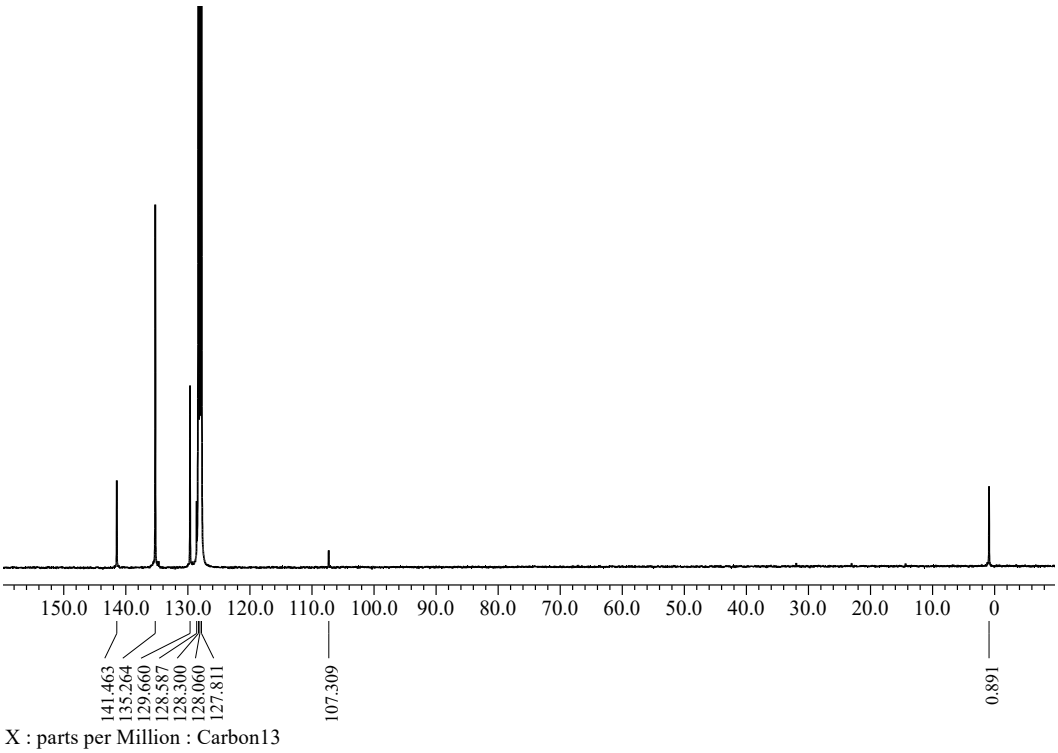

Figure S2. ^{13}C NMR spectrum (C_6D_6, 100 MHz) of $\mathbf{1_{Sn}}$

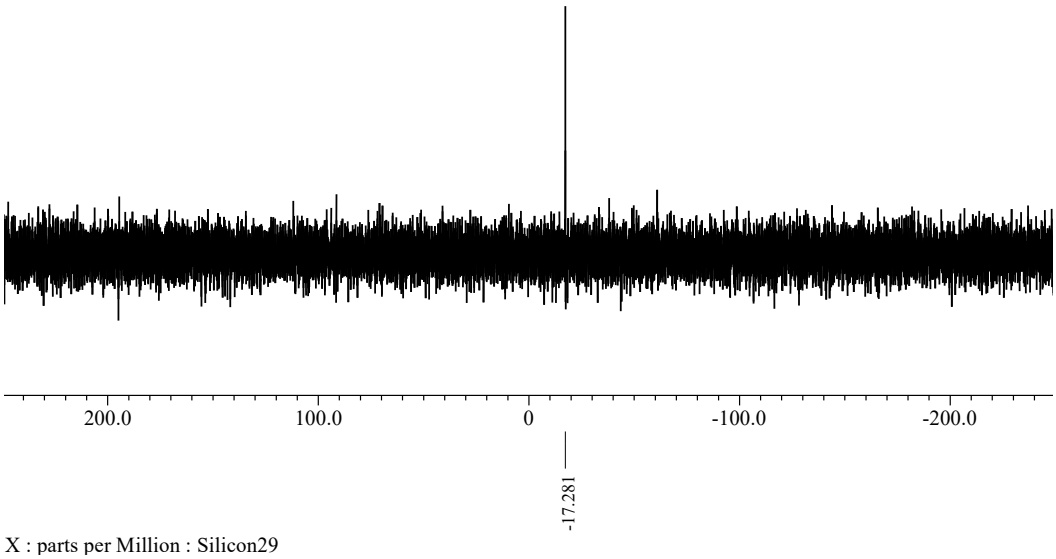

Figure S3. ^{29}Si NMR spectrum (C_6D_6, 79 MHz) of $\mathbf{1_{Sn}}$

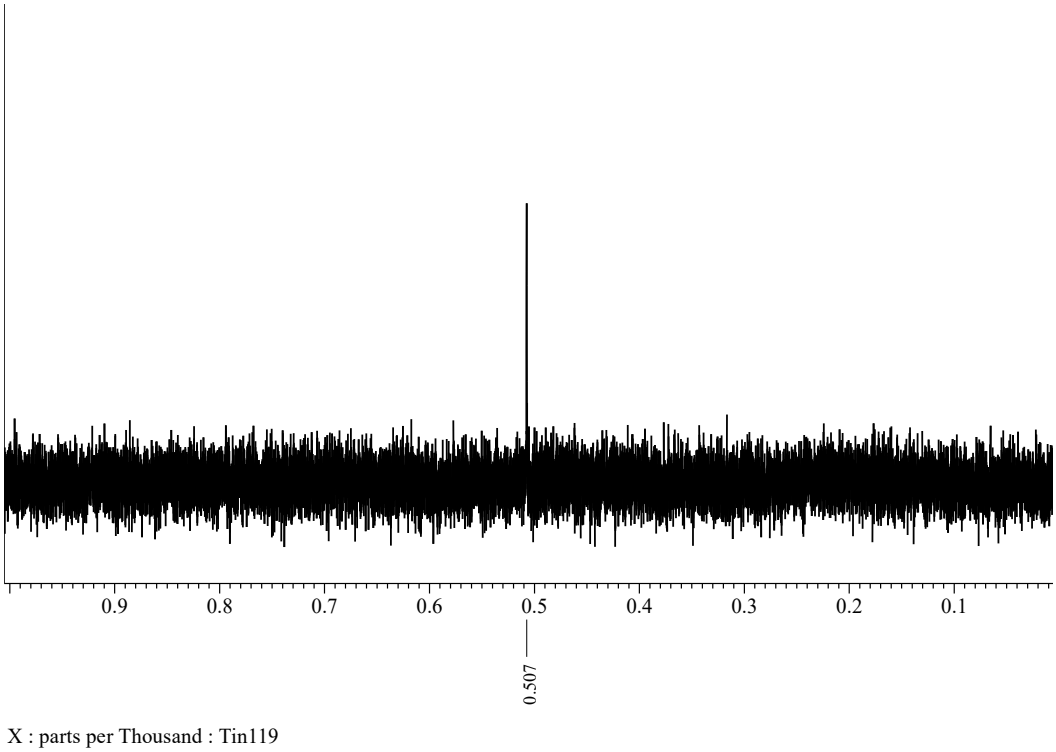

Figure S4. ^{119}Sn NMR spectrum (C_6D_6, 148 MHz) of $\mathbf{1_{Sn}}$

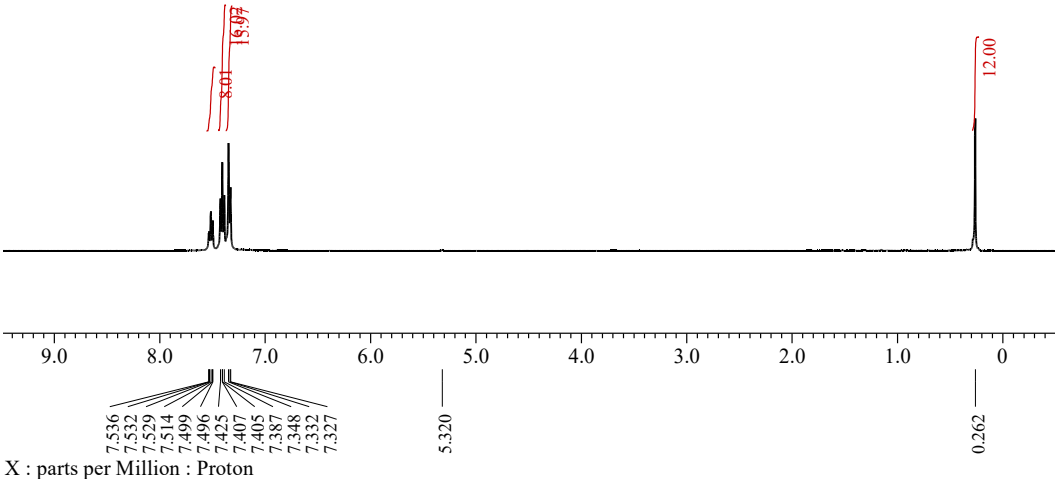

Figure S5. ^{1}H NMR spectrum (CD_2Cl_2, 400 MHz) of $\mathbf{1_{Sn}}$

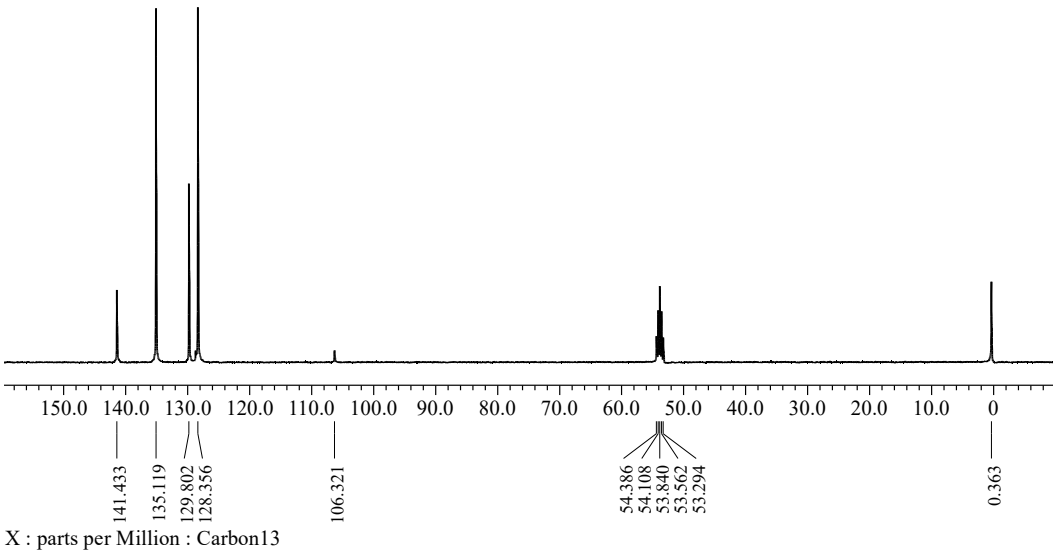

Figure S6. ^{13}C NMR spectrum (CD_2Cl_2, 100 MHz) of $\mathbf{1_{Sn}}$

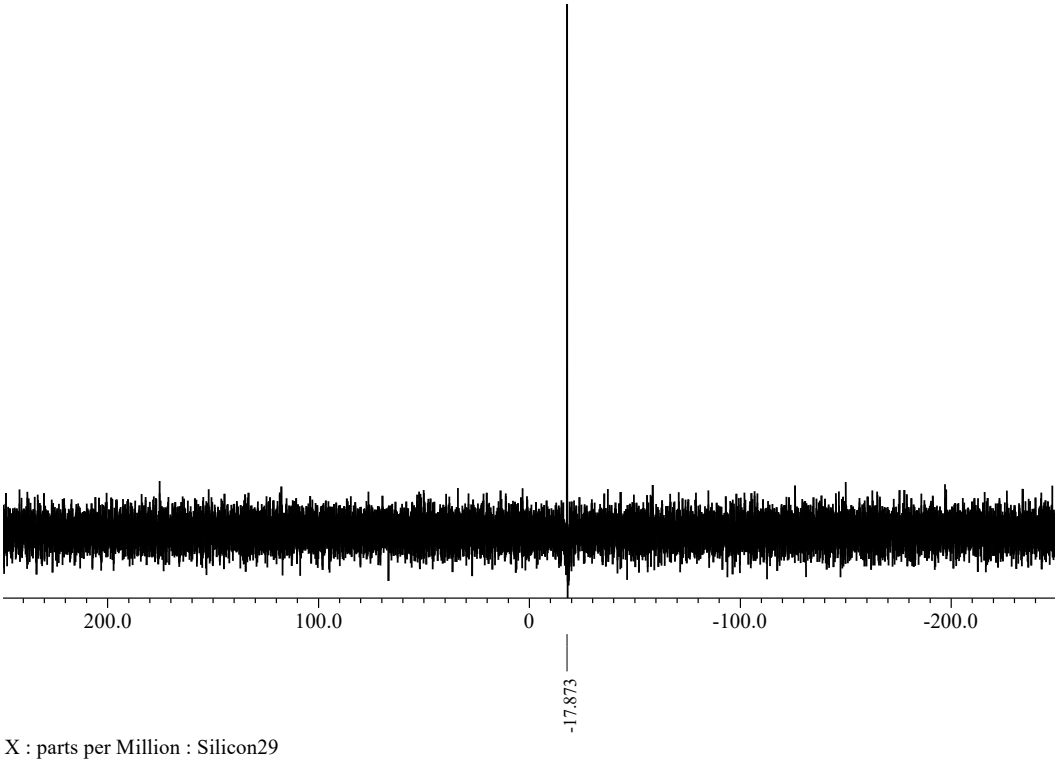

Figure S7. ^{29}Si NMR spectrum (CD_2Cl_2, 79 MHz) of $\mathbf{1_{Sn}}$

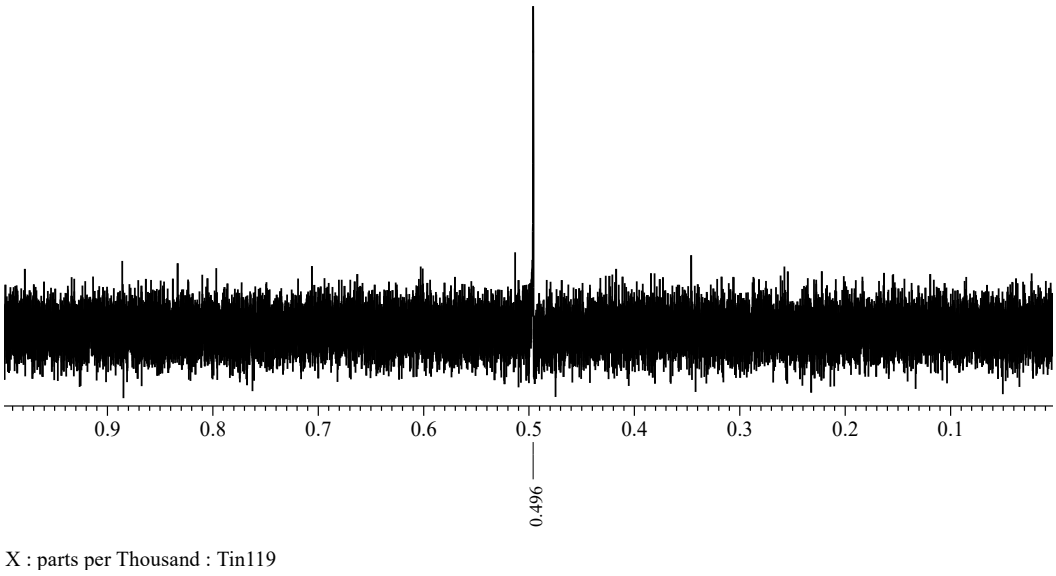

Figure S8. ^{119}Sn NMR spectrum (CD_2Cl_2, 148 MHz) of $\mathbf{1_{Sn}}$

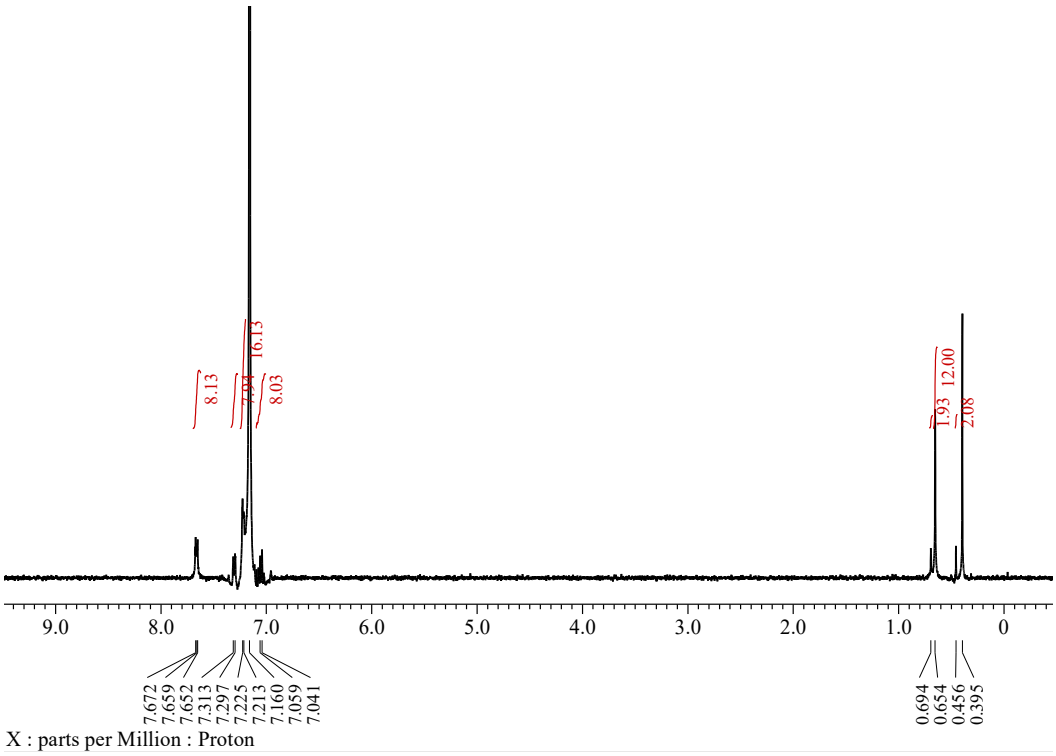

Figure S9. ^{1}H NMR spectrum (C_6D_6, 400 MHz) of **2**

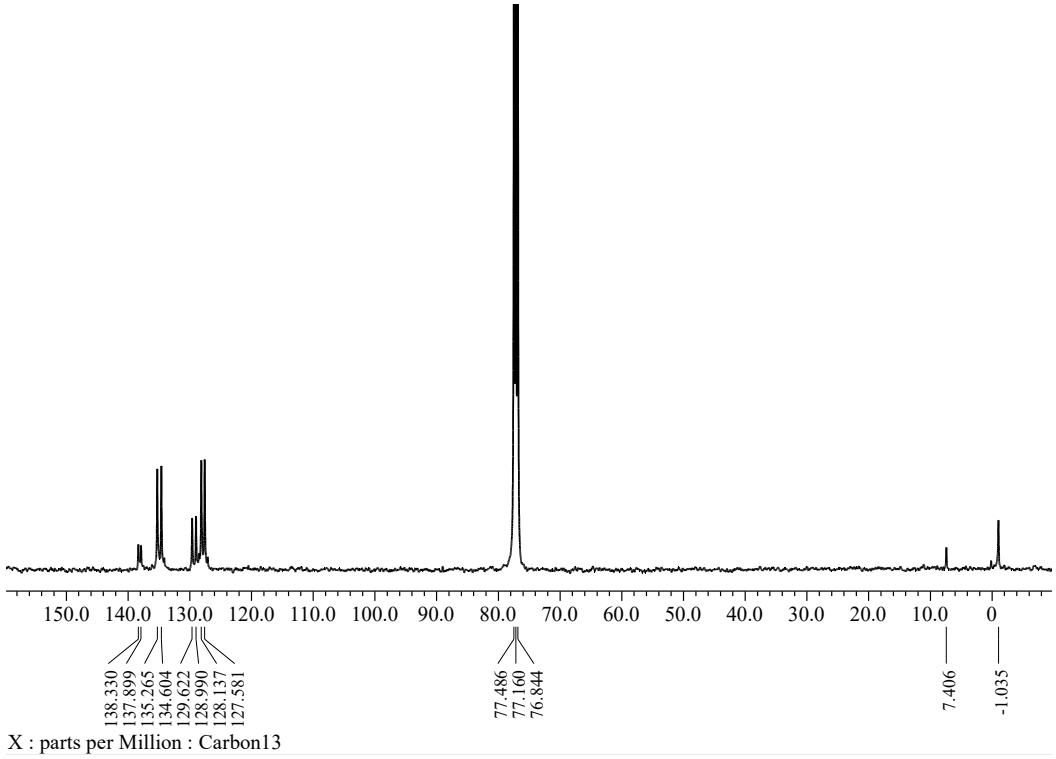

Figure S10. ^{13}C NMR spectrum ($CDCl_3$, 100 MHz) of **2**

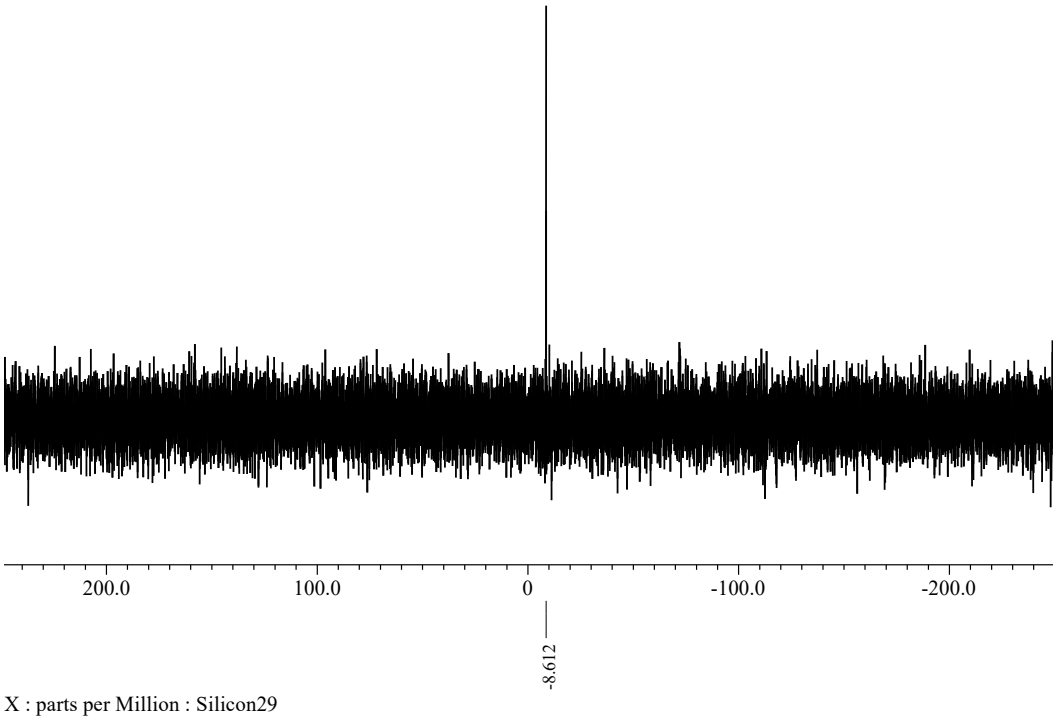

Figure S11. ^{29}Si NMR spectrum (C_6D_6, 79 MHz) of **2**

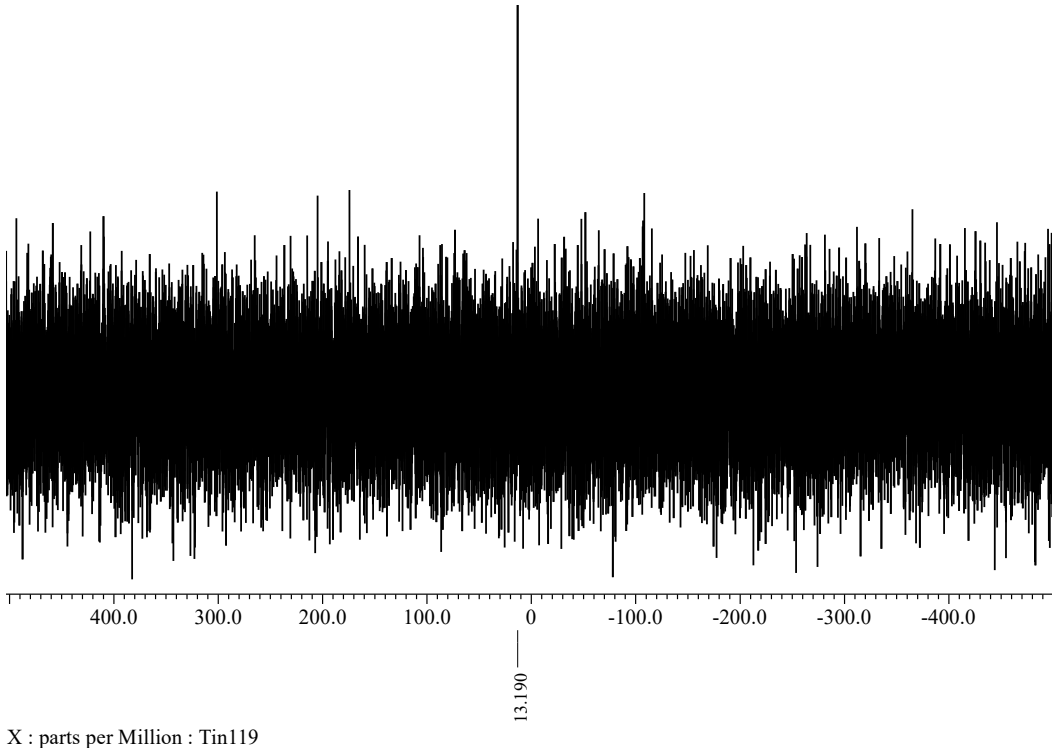

Figure S12. ^{119}Sn NMR spectrum (C_6D_6, 148 MHz) of **2**

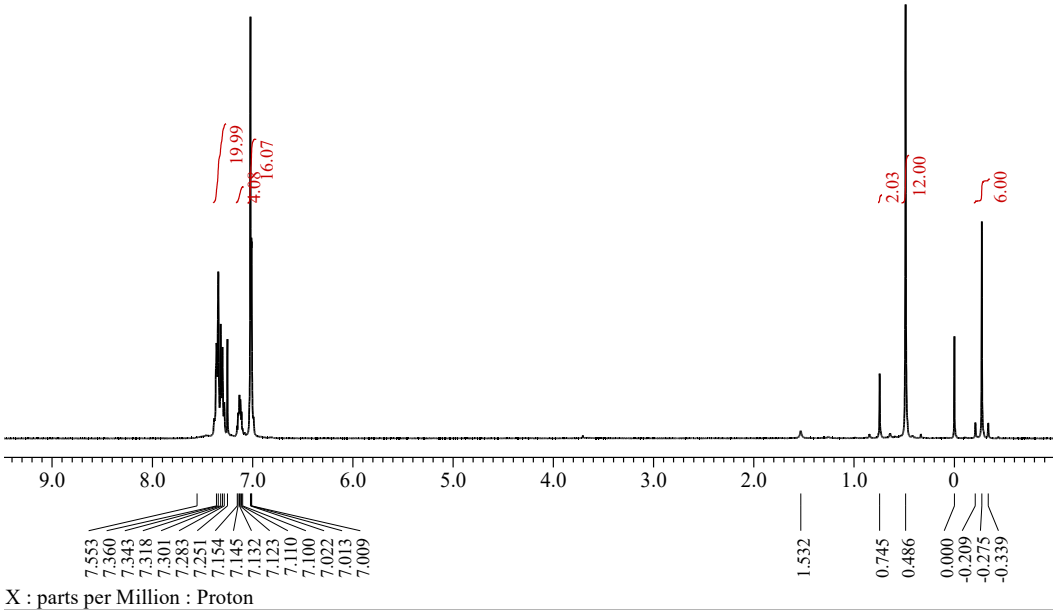

Figure S13. ^{1}H NMR spectrum ($CDCl_3$, 400 MHz) of **3**

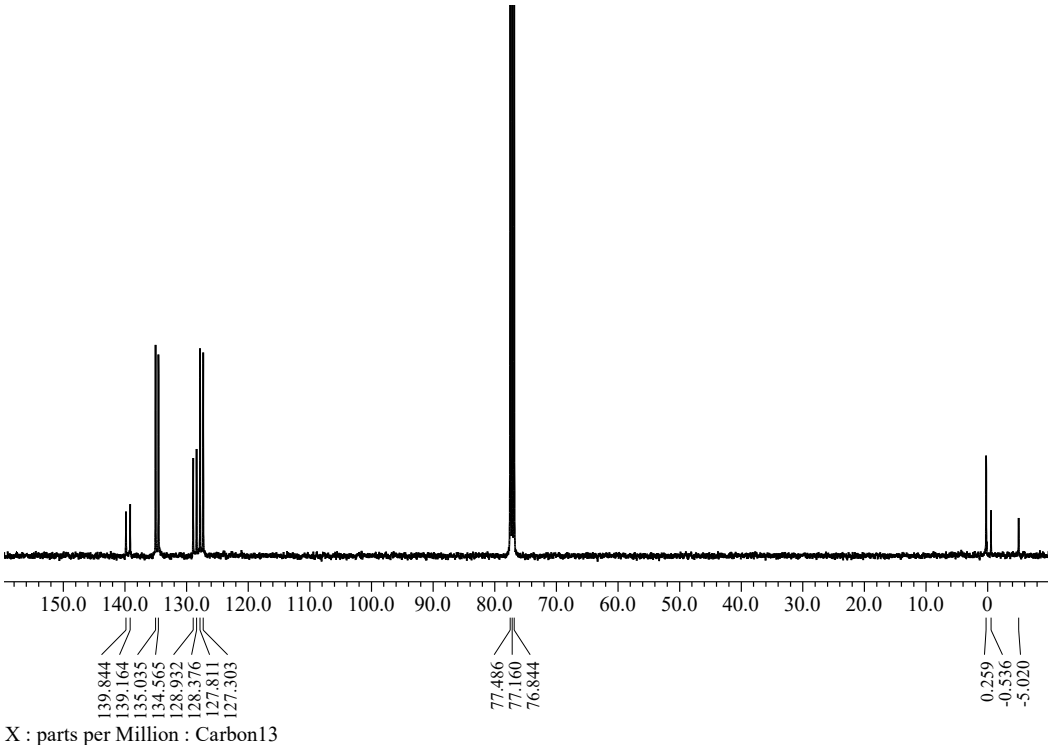

Figure S14. ^{13}C NMR spectrum ($CDCl_3$, 100 MHz) of **3**

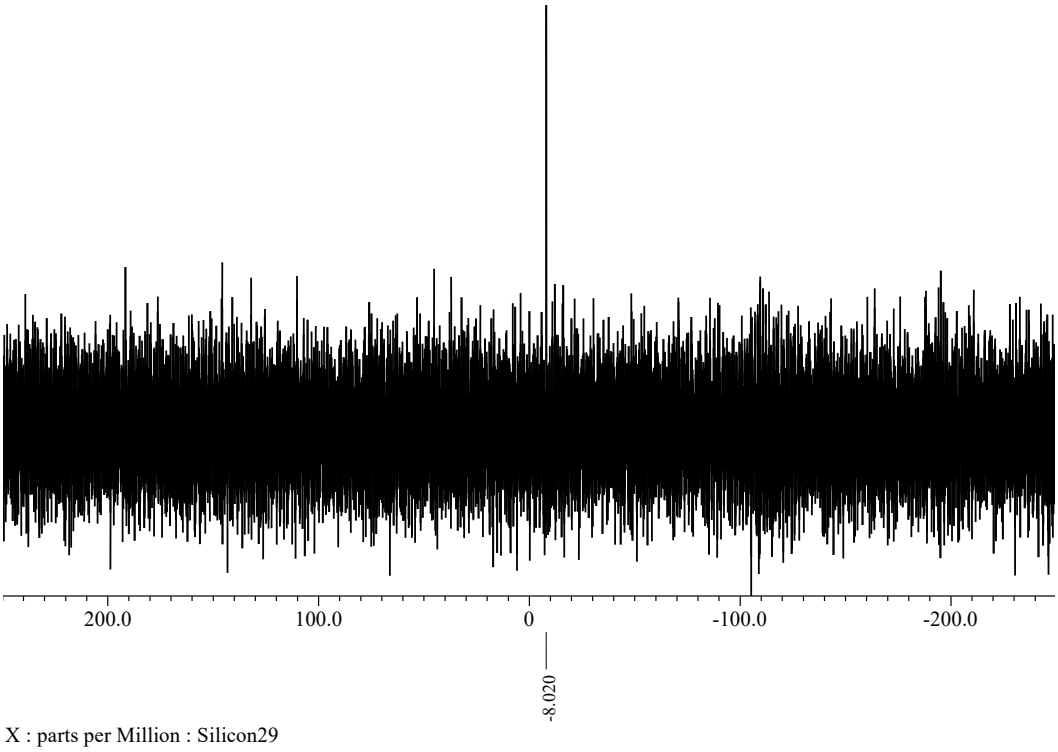

Figure S15. ^{29}Si NMR spectrum ($CDCl_3$, 79 MHz) of **3**

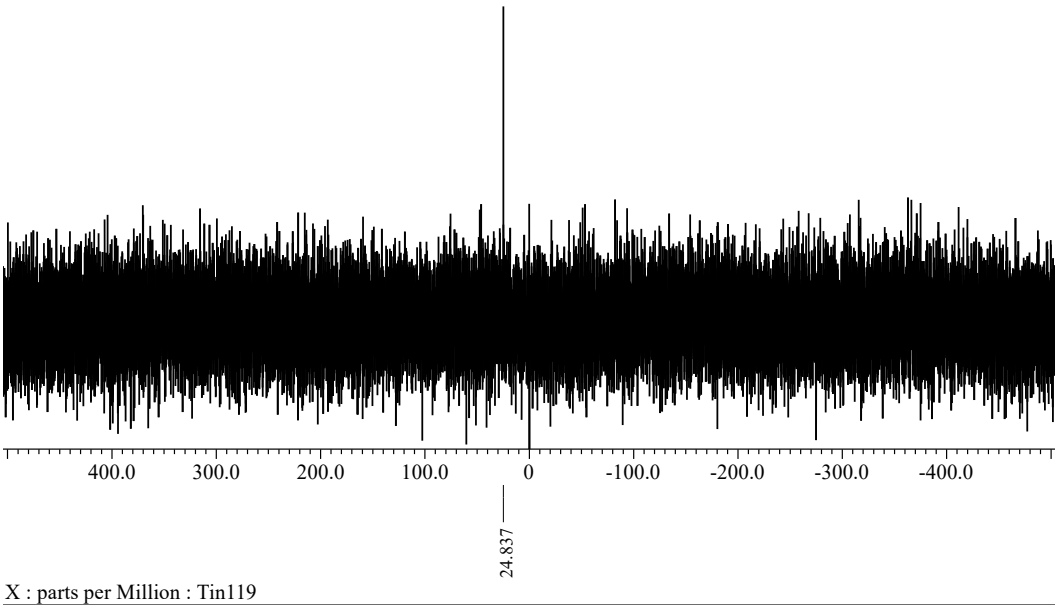

Figure S16. ^{119}Sn NMR spectrum ($CDCl_3$, 148 MHz) of **3**

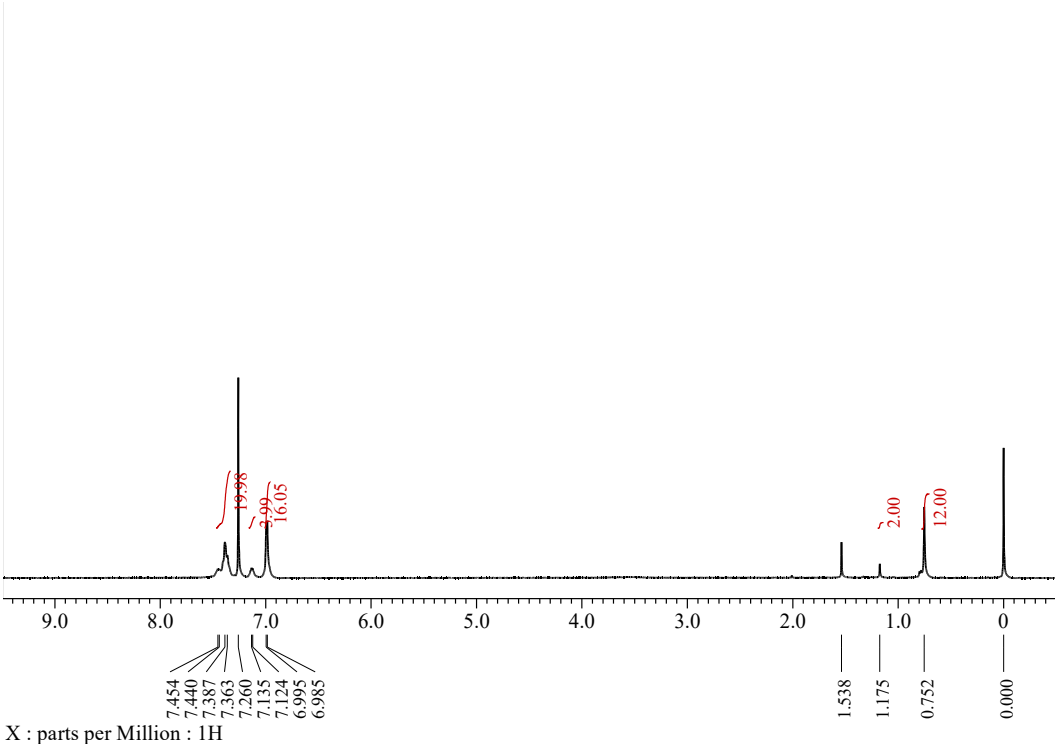

Figure S17. ^{1}H NMR spectrum ($CDCl_3$, 400 MHz) of **4Cl**

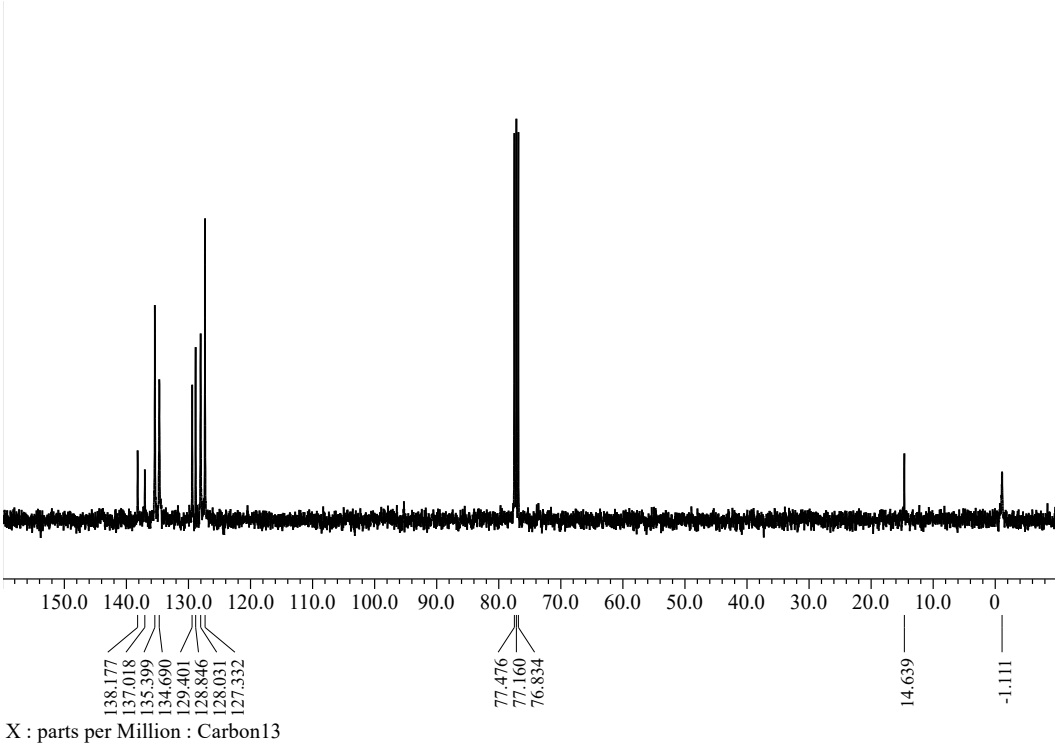

Figure S18. ^{13}C NMR spectrum ($CDCl_3$, 100 MHz) of **4Cl**

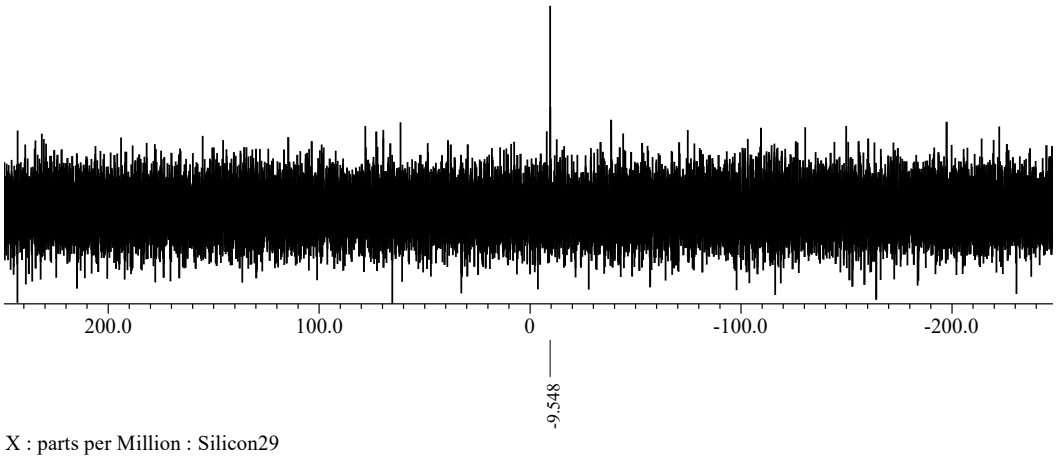

Figure S19. ^{29}Si NMR spectrum ($CDCl_3$, 79 MHz) of **4Cl**

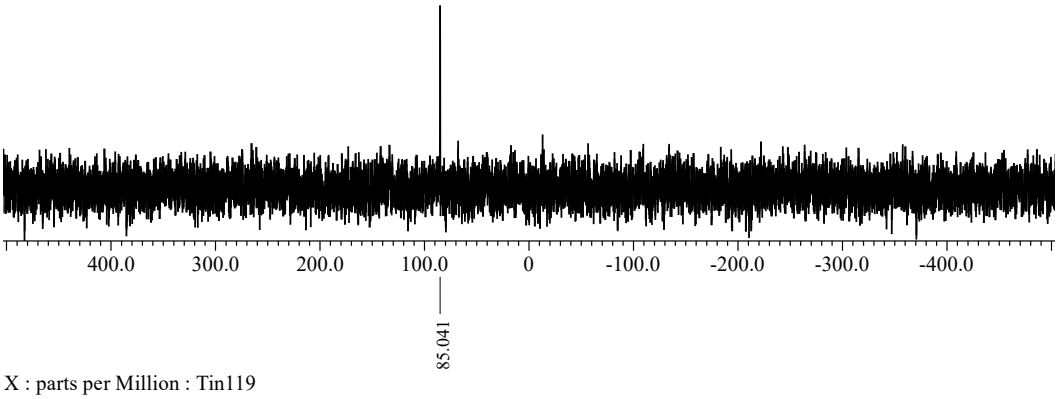

Figure S20. ^{119}Sn NMR spectrum ($CDCl_3$, 148 MHz) of **4Cl**

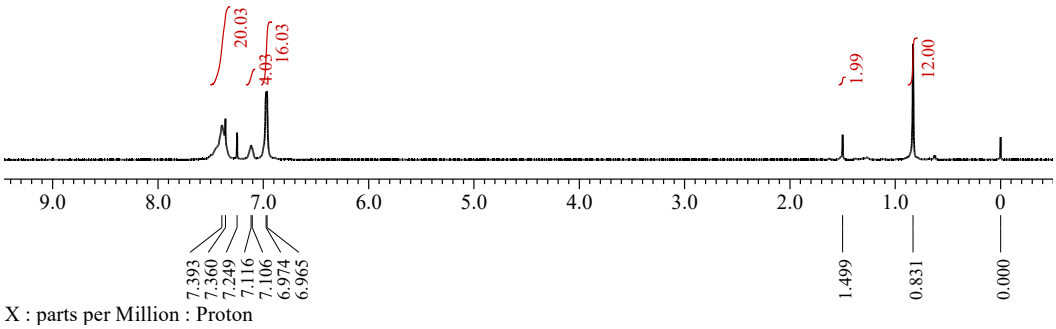

Figure S21. ^{1}H NMR spectrum ($CDCl_3$, 400 MHz, 298 K) of **4Br**

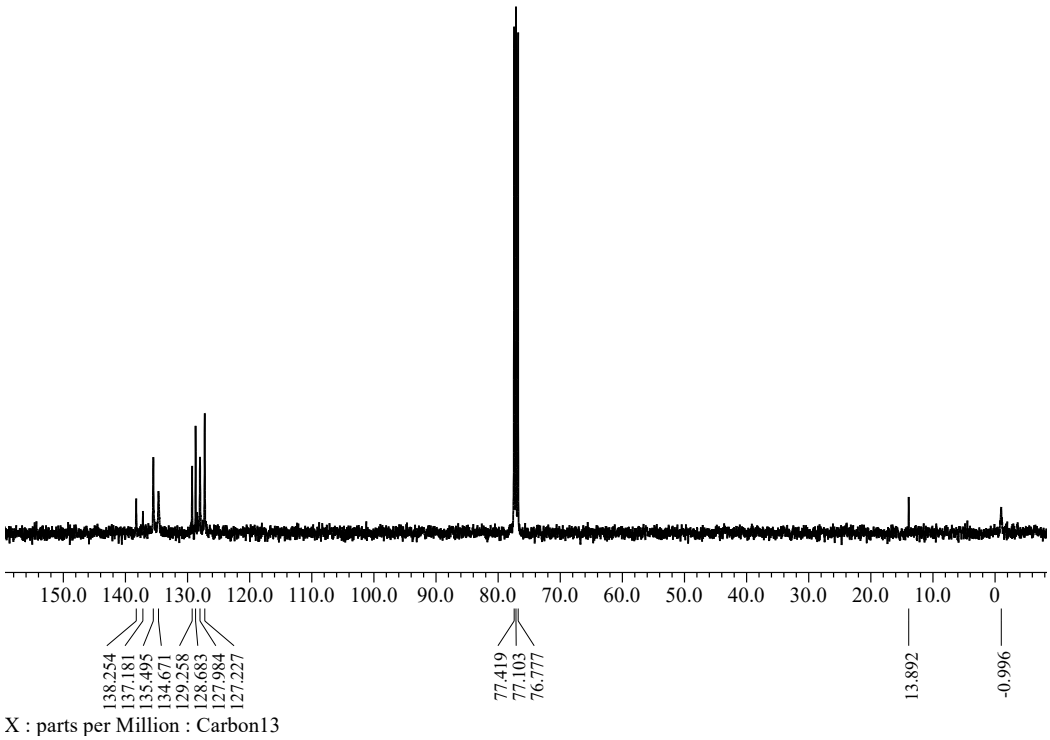

Figure S22. ^{13}C NMR spectrum ($CDCl_3$, 100 MHz, 298 K) of **4Br**

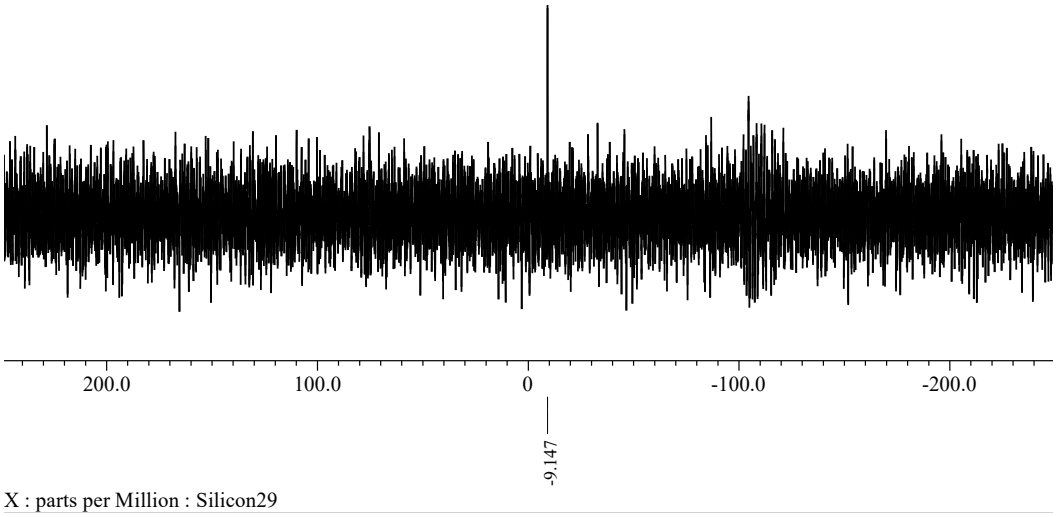

Figure S23. ^{29}Si NMR spectrum ($CDCl_3$, 79 MHz, 298 K) of **4Br**

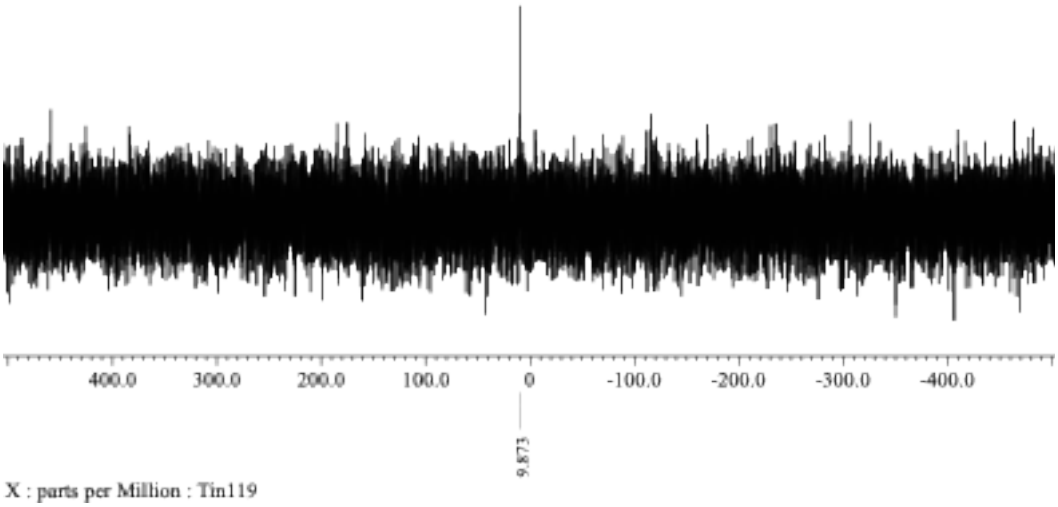

Figure S24. ^{119}Sn NMR spectrum ($CDCl_3$, 148 MHz, 298 K) of **4Br**

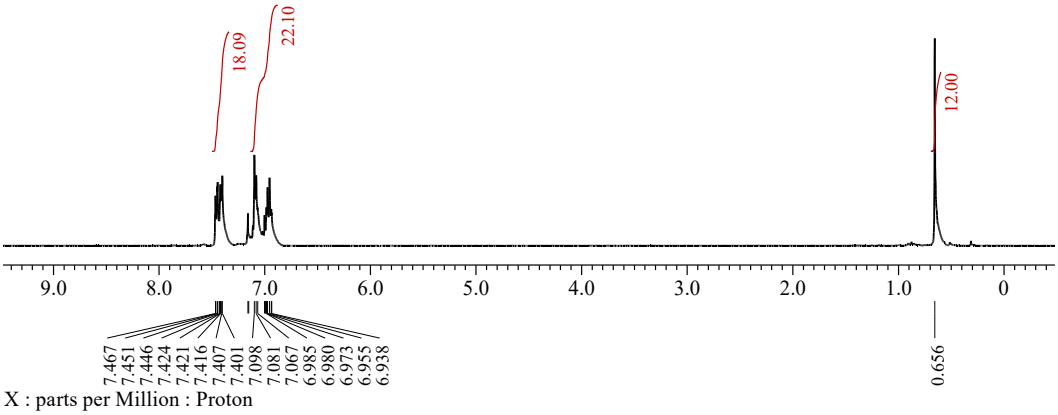

Figure S25. ^{1}H NMR spectrum (C_6D_6, 400 MHz) of **5Cl**

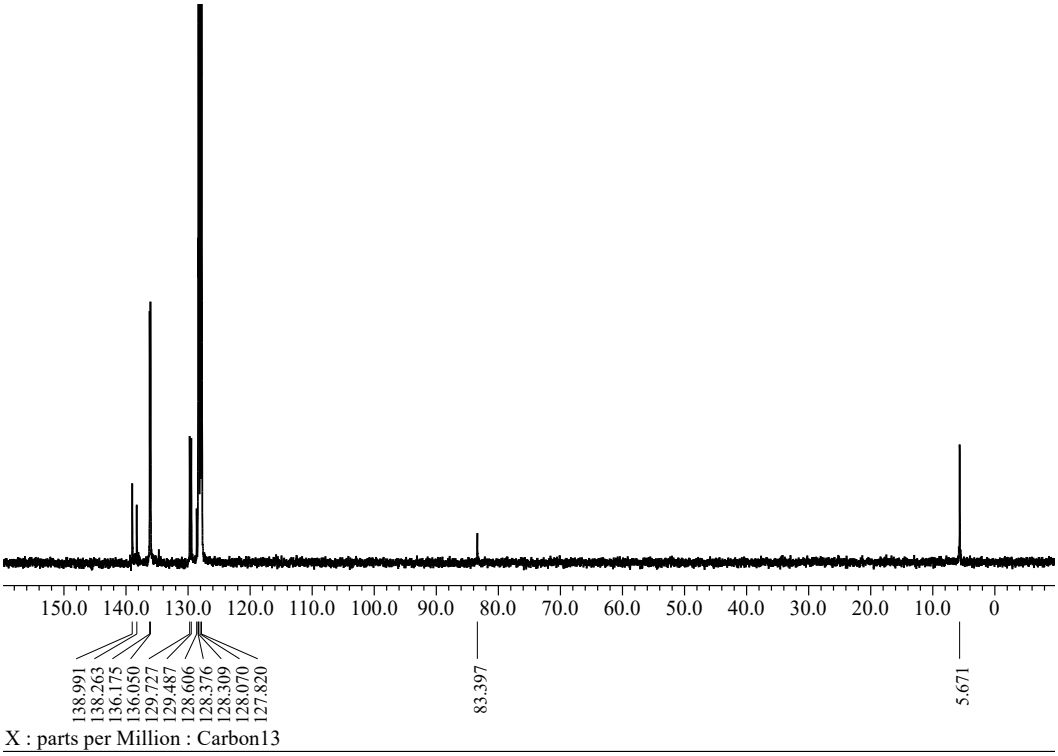

Figure S26. ^{13}C NMR spectrum (C_6D_6, 100 MHz) of **5Cl**

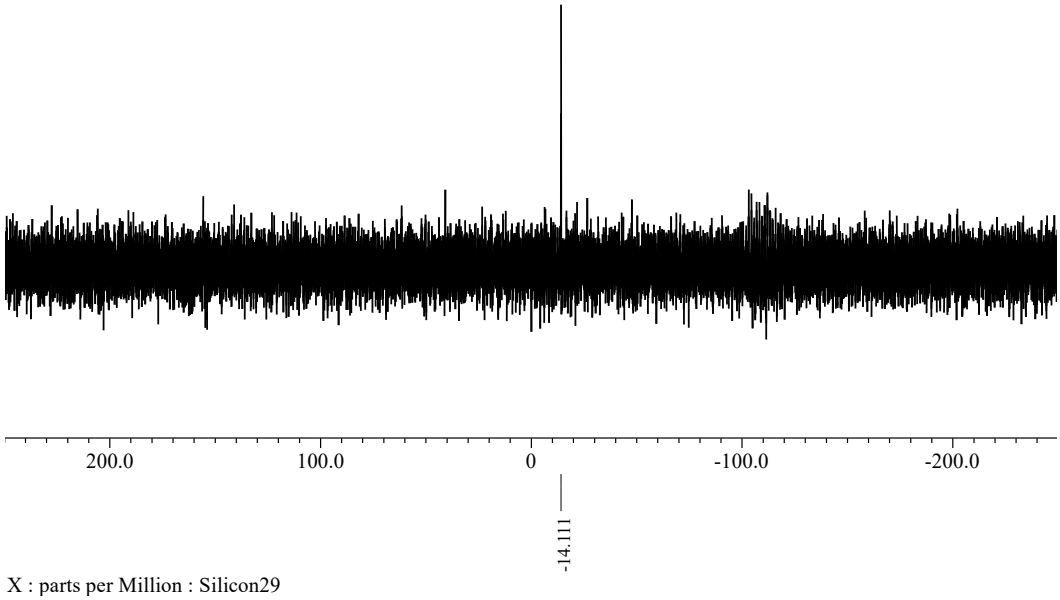

Figure 27. ^{29}Si NMR spectrum (C_6D_6, 79 MHz) of **5Cl**

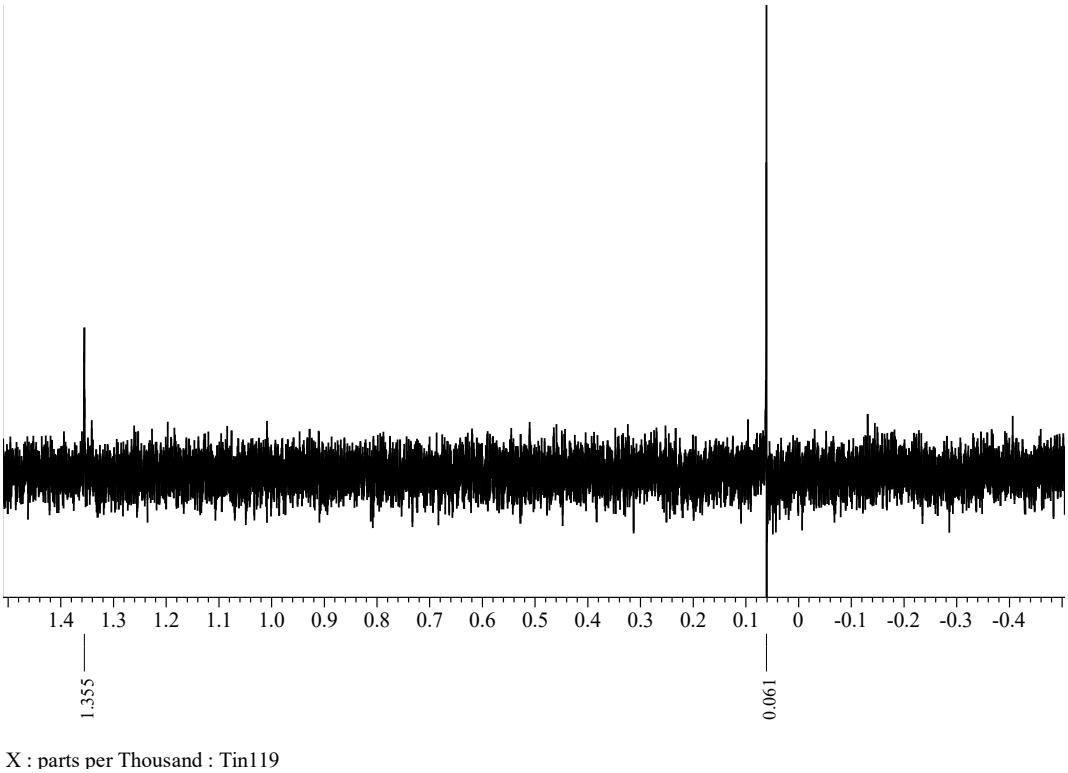

Figure S28. ^{119}Sn NMR spectrum (C_6D_6, 148 MHz) of **5Cl**

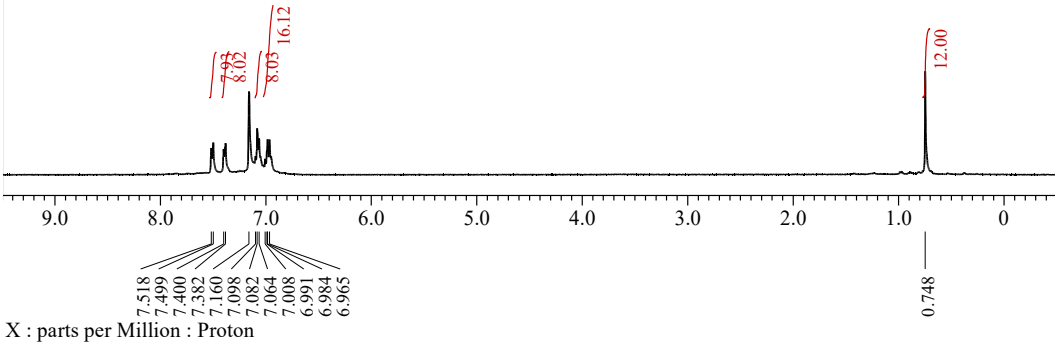

Figure S29. ^{1}H NMR spectrum (C_6D_6, 400 MHz) of **5Br**

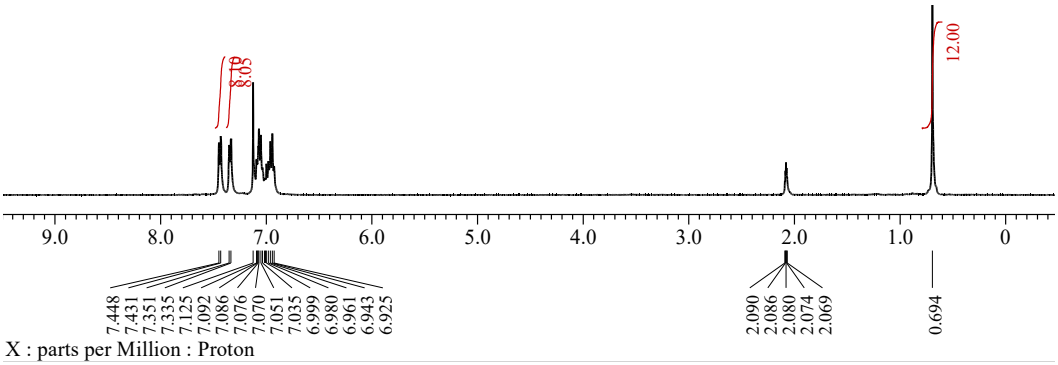

Figure S30. ^{1}H NMR spectrum (toluene-d_8, 400 MHz) of **5Br**

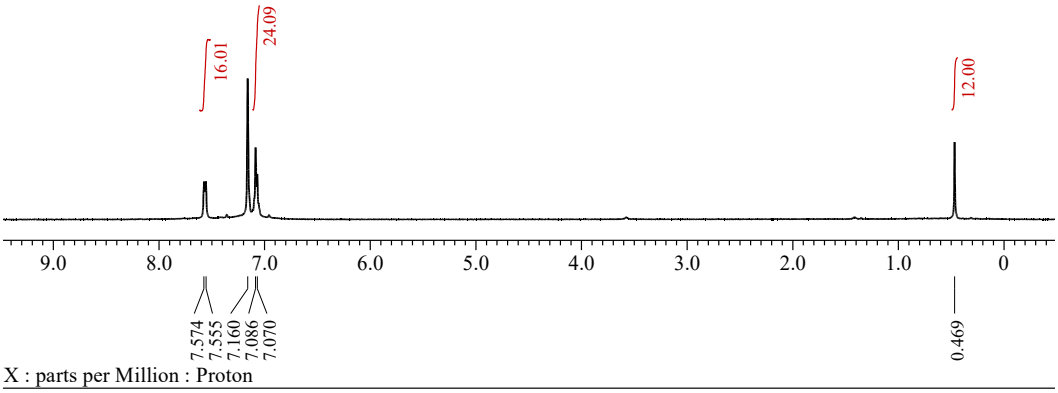

Figure S31. ^{1}H NMR spectrum (C_6D_6, 400 MHz, 298 K) of **6**

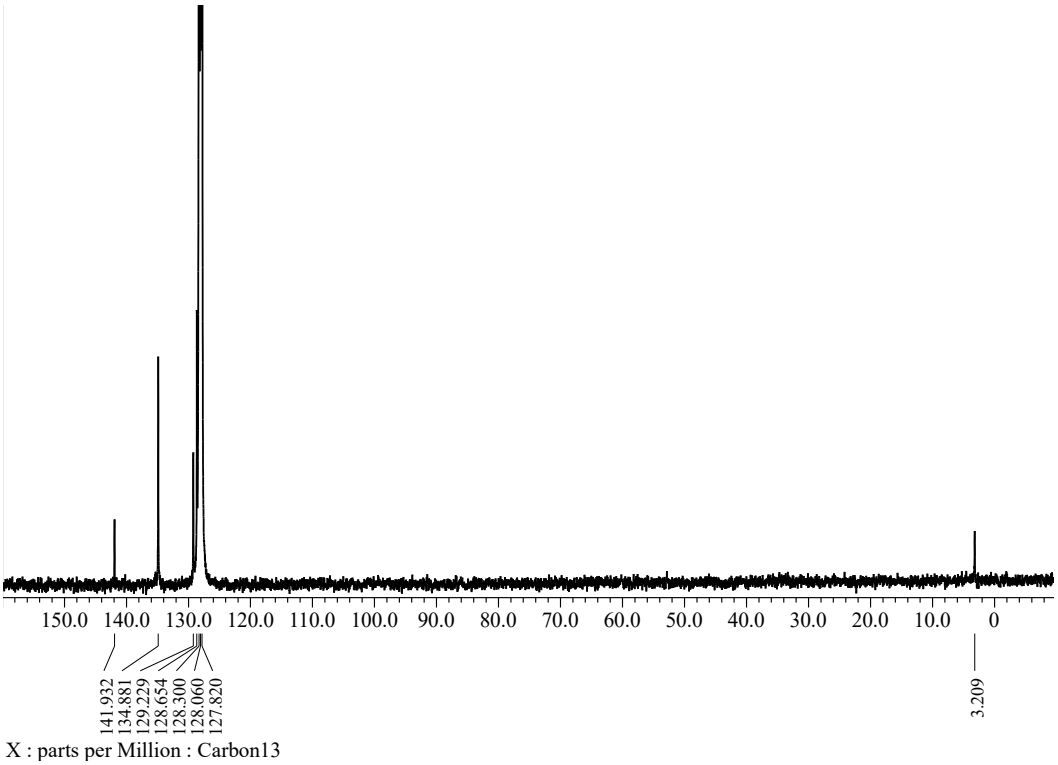

Figure S32. ^{13}C NMR spectrum (C_6D_6, 100 MHz, 298 K) of **6**

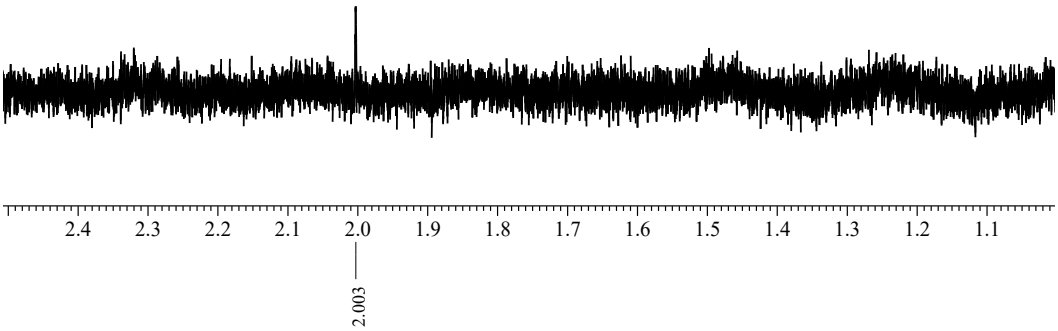

X : parts per Thousand : Tin119

Figure S33. ^{119}Sn NMR spectrum (C_6D_6, 148 MHz, 348 K) of **6**

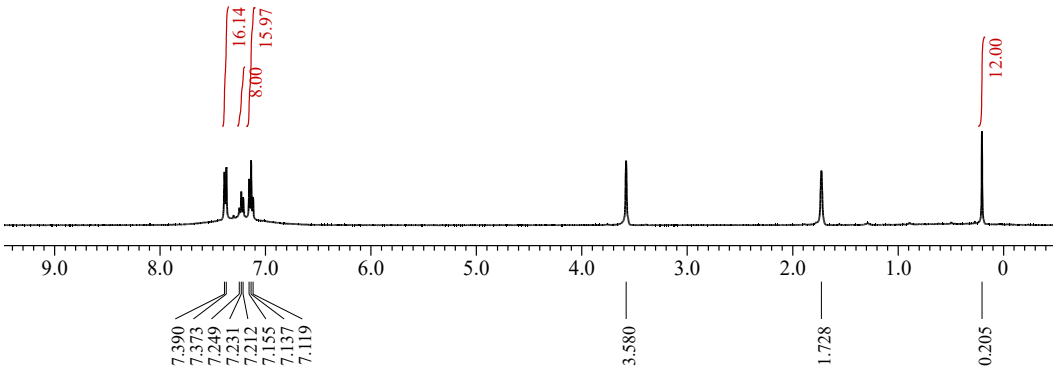

X : parts per Million : Proton

Figure S34. ^{1}H NMR spectrum (tetrahydrofurane-d_8, 400 MHz, 298 K) of **6**

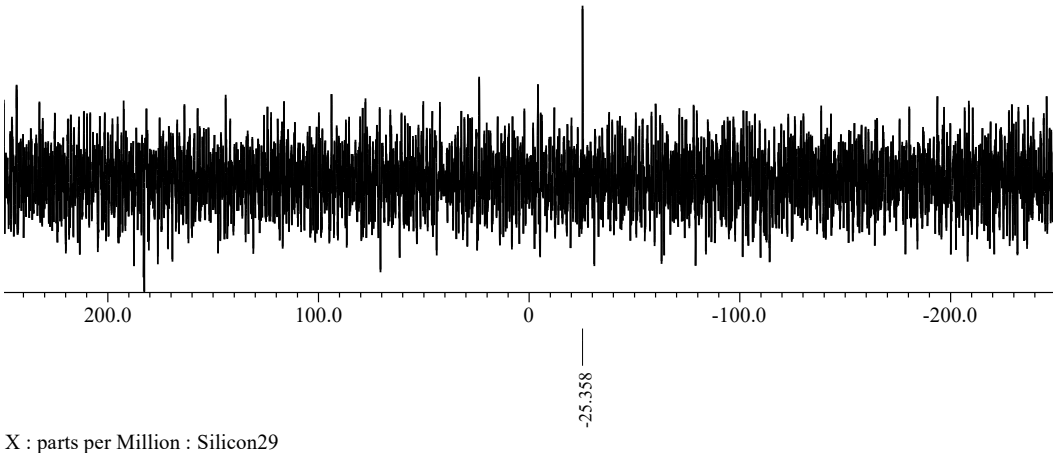

Figure S35. ^{29}Si NMR spectrum (tetrahydrofurane-d_8, 79 MHz, 298 K) of **6**

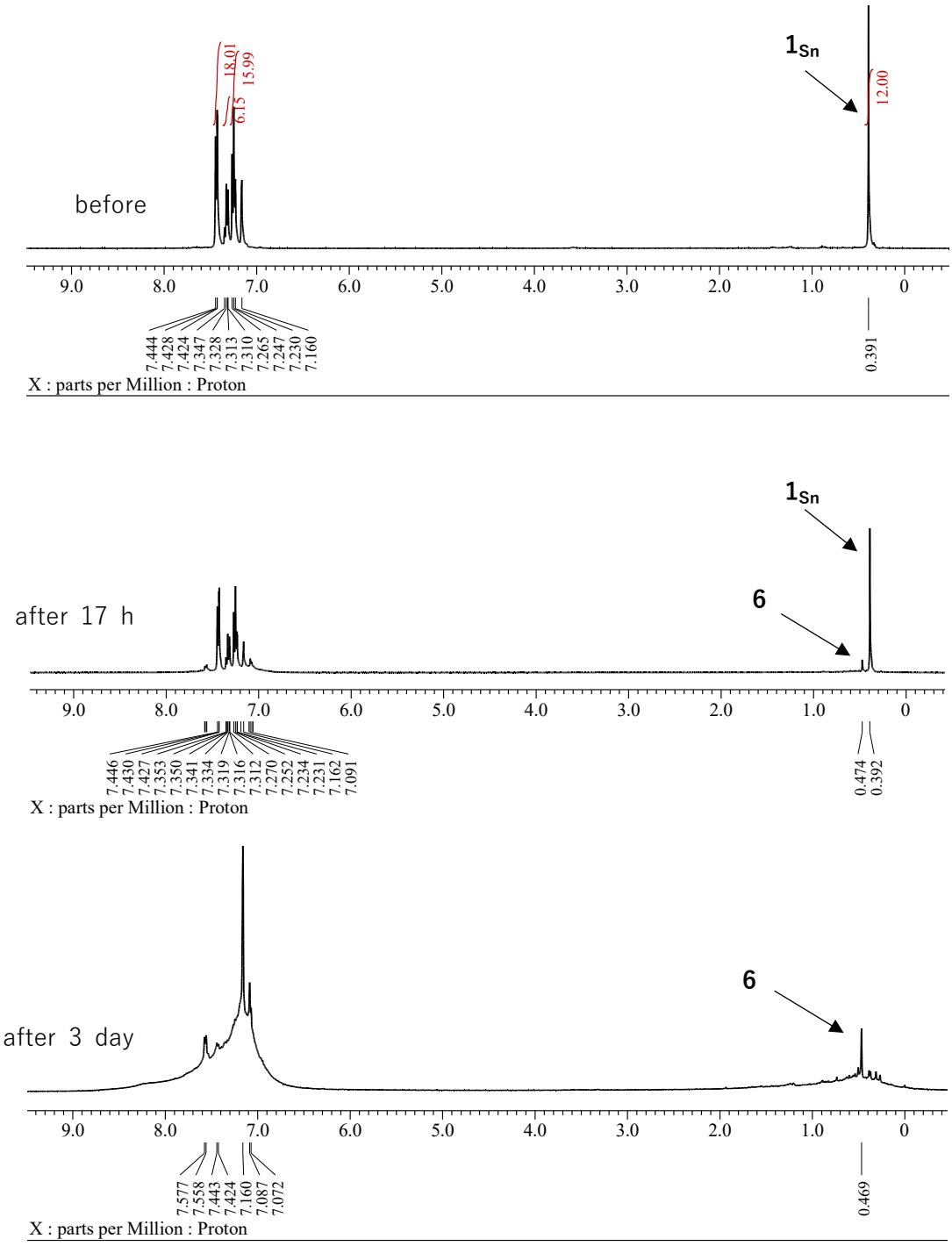

Figure S36. ^{1}H NMR spectrum (C_6D_6, 79 MHz, 298 K) of photoreaction of $\mathbf{1_{Sn}}$

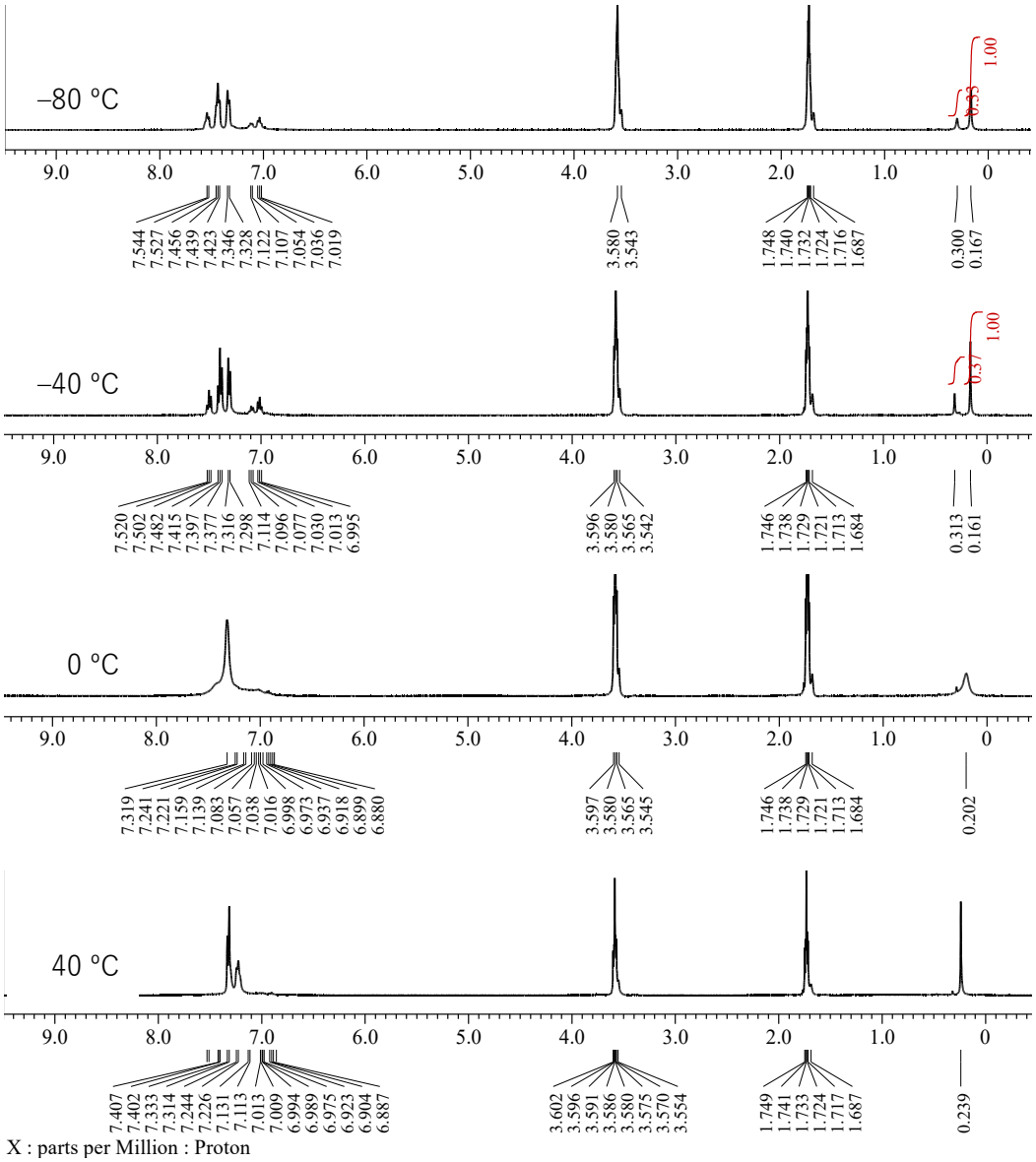

Figure S37. Variable temperature ^{1}H NMR spectra of $\mathbf{1_{Sn}}$ (tetrahydrofurane-d_8, 400 MHz).

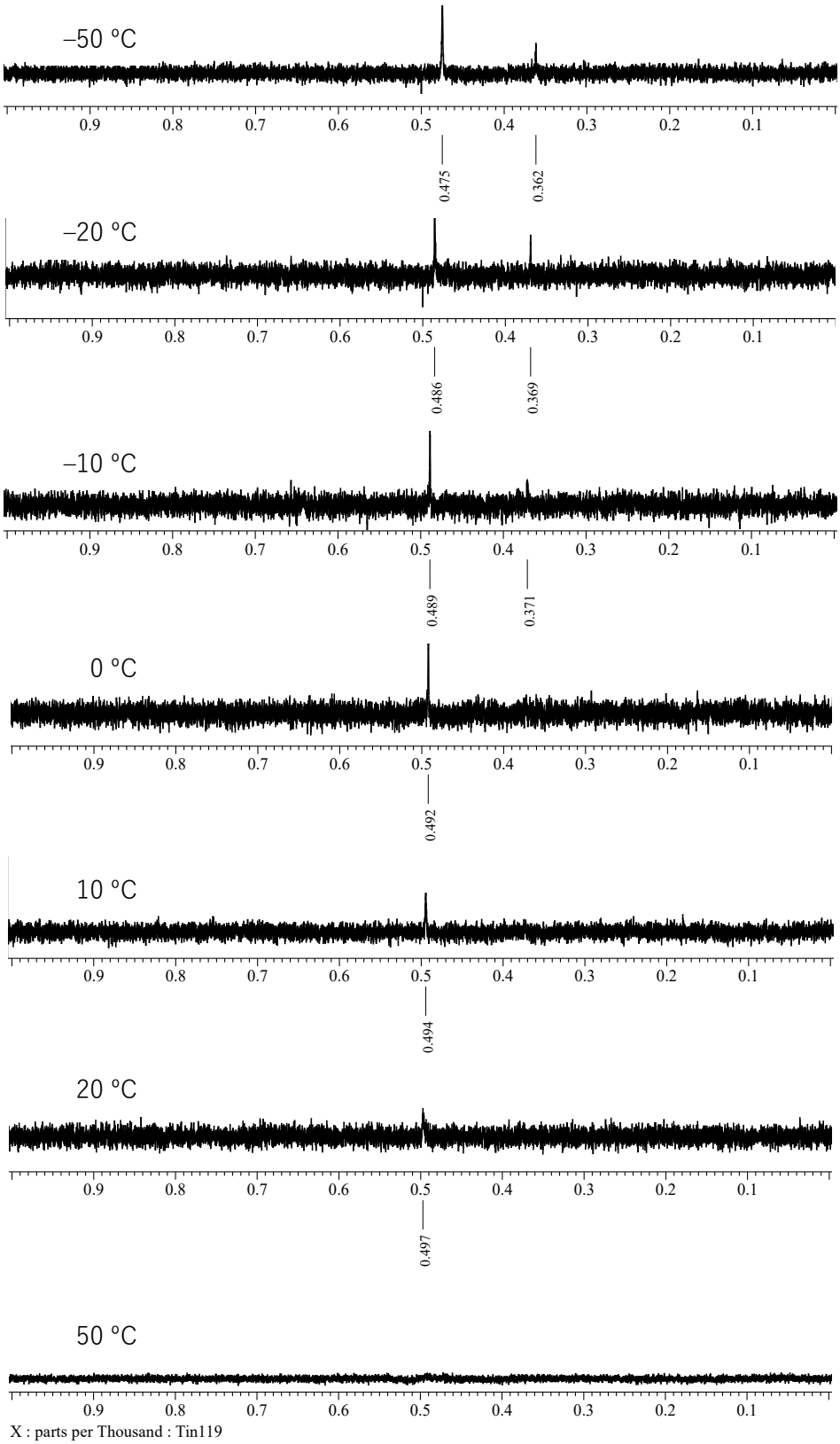

Figure S38. Variable temperature ^{119}Sn NMR spectra of $\mathbf{1_{Sn}}$ (tetrahydrofurane, 148 MHz).

X-ray Crystallographic Analysis

Suitable single crystals **1-3**, **5X**, and **6** were grown by slow recrystallization from organic solvents at room temperature as shown in Table S1. Single-crystal X-ray diffraction (SC-XRD) data of **1-3**, **5Br**, and **6** were collected at 100 K using a Bruker-D8 Quest diffractometer equipped with a PHOTON detector, and Graphite monochromated Mo Kα radiation (λ = 0.7103 Å) IμS microfocus source. The diffraction data for **5Cl** was collected at the BL02B1 beamline of Spring-8 on Piratus3 X Ditector (Dectris) using synchrotron radiation The structures were determined by intrinsic phasing (SHELXT 2018/2)[S1] and refined by full-matrix least-squares refinement (SHELXL-2018/3)[S2] using the yadokari[S3] software package. Refinement results are summarized in Tables S1. Deposition numbers 2288706 (**1**), 2288707 (**2**), 2288708 (**3**), 2288705 (**5Cl**), 2305276 (**5Br**), and 2305277 (**6**) contain the supplementary crystallographic data for this paper. The data can be obtained free of charge via www.ccdc.cam.ac.uk/data_request/cif (or from the Cambridge Crystallographic Data Centre, 12 Union Road, Cambridge CB2 1EZ, U.K.).

Table S1. Crystal data and data collection of **1-3, 5X**, and **6**.

Compound	$\mathbf{1_{Sn}}$	**2**	**3**	**5Cl**	**5Br**	**6**
solvent	C_6H_6 / Hexane	C_6H_6 / Hexane	C_6H_6 / Hexane	C_6H_6 / Hexane	C_6H_6 / Hexane	THF
Empirical formula	$C_{54}H_{52}Si_4Sn$	$C_{54}H_{56}O_2Si_4Sn$	$C_{56}H_{60}Si_4Sn$	$C_{54}H_{52}Cl_2Si_4Sn_2 \cdot 2.5C_6H_6$	$C_{54}H_{52}Br_2Si_4Sn_2 \cdot 2.5C_6H_6$	$C_{54}H_{52}Si_4Sn_2$
Formula weight	932.00	968.03	964.09	1316.86	1405.78	1050.69
Temperature (K)	110(2)	110(2)	100(2)	100(2)	100(2)	100(2)
Wavelength (Å)	0.71073	0.71073	0.71073	0.4139	0.71073	0.71073
Crystal system	Monoclinic	Triclinic	Triclinic	Monoclinic	Monoclinic	Triclinic
Space group	$P2_1/c$	P-1	P-1	$P2_1/c$	$P2_1/c$	P-1
Unit cell dimensions						
a (Å)	10.8346(2)	11.2316(3)	11.5084(4)	14.6488(1)	14.5967(5)	10.0462(4)
b (Å)	15.7565(3)	12.9893(4)	13.1355(5)	23.2014(2)	23.3500(8)	10.6969(4)
c (Å)	26.9143(5)	17.5630(5)	17.4215(7)	18.0516(1)	18.0604(6)	12.2851(3)
α (°)	90	70.964(3)	71.074(4)	90	90	81.137(2)
β (°)	90.212(2)	75.647(3)	75.050(4)	95.193(1)	94.819(3)	74.219(3)
γ (°)	90	84.203(3)	84.125(3)	90	90	66.744(4)
Volume (Å^3)	4594.65(15)	2345.99(13)	2406.38(17)	6110.06(8)	6133.8(4)	1165.58(8)
Z	4	2	2	4	4	1
Density (g/cm^3)	1.347	1.370	1.331	1.432	1.522	1.497
Data / restraints / parameters	10518 / 0 / 536	10754 / 0 / 556	11021 / 0 / 556	14000 / 0 / 698	12523 / 39 / 698	5308 / 0 / 273
Goodness-of-fit on F^2	1.044	1.028	1.059	1.053	1.103	1.046
R_1, wR_2	0.0243, 0.0733	0.0264, 0.0614	0.0270, 0.0556	0.0233, 0.0623	0.0504, 0.1049	0.0166, 0.0436
CCDC Number	2288706	2288707	2288708	2288705	2305276	2305277

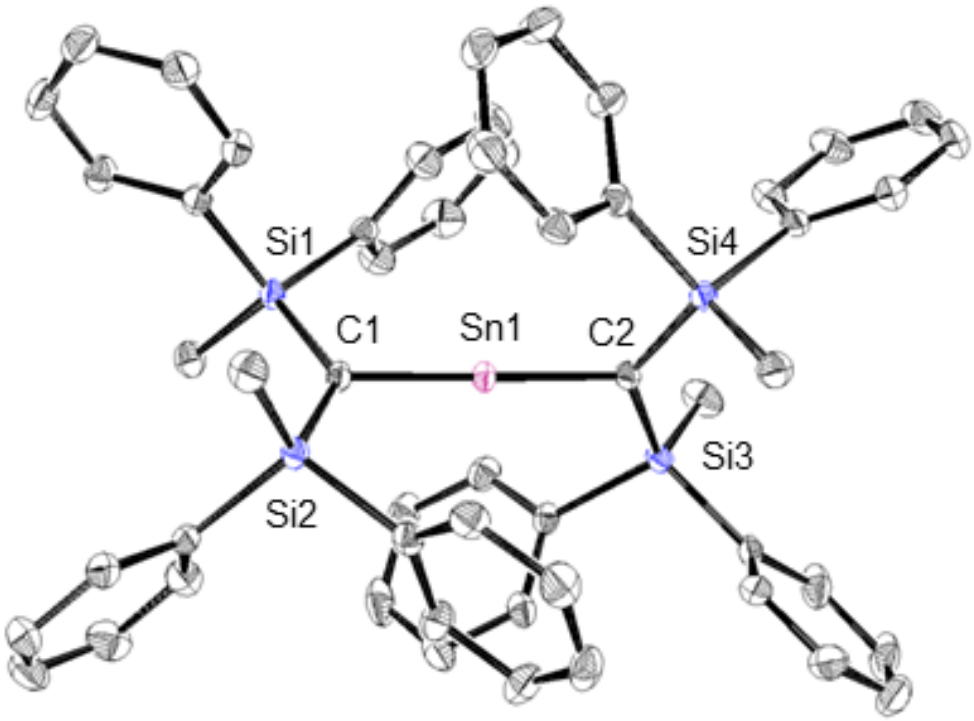

Figure S39. Structure of $\mathbf{1_{Sn}}$

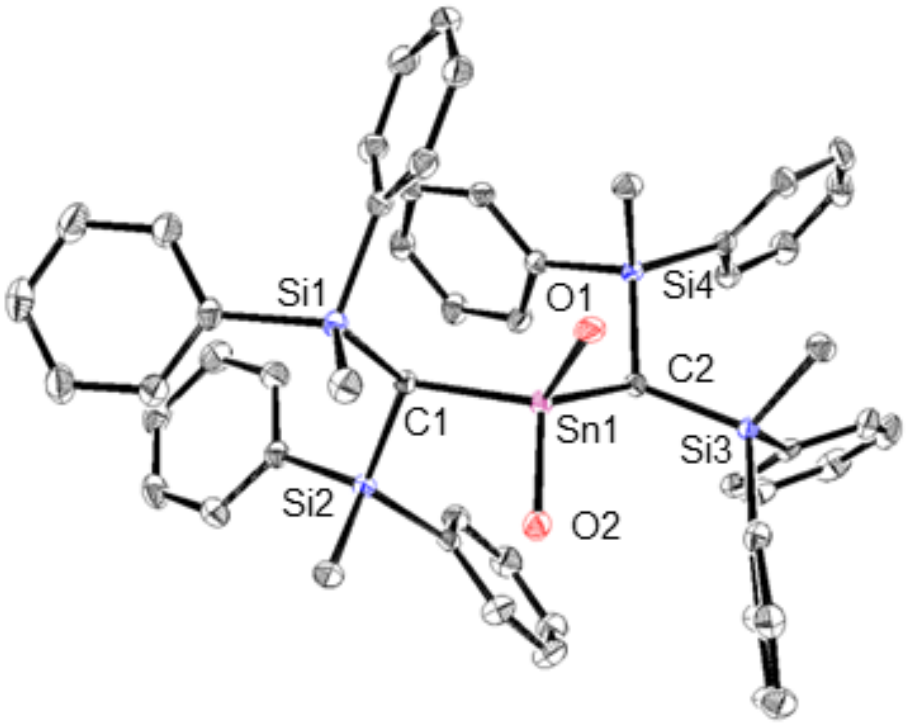

Figure S40. Structure of **2**

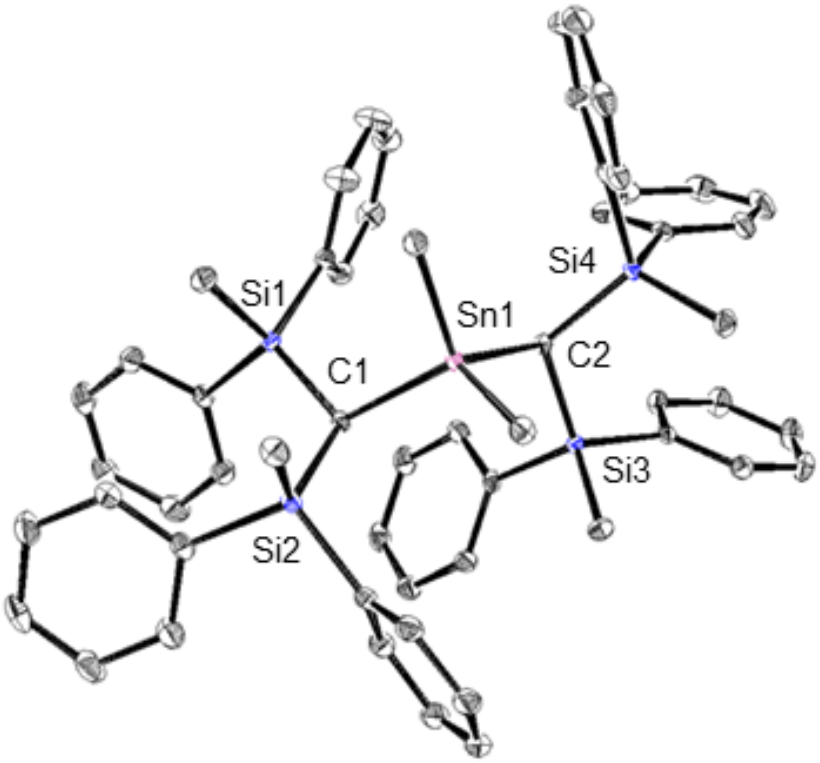

Figure S41. Structure of **3**

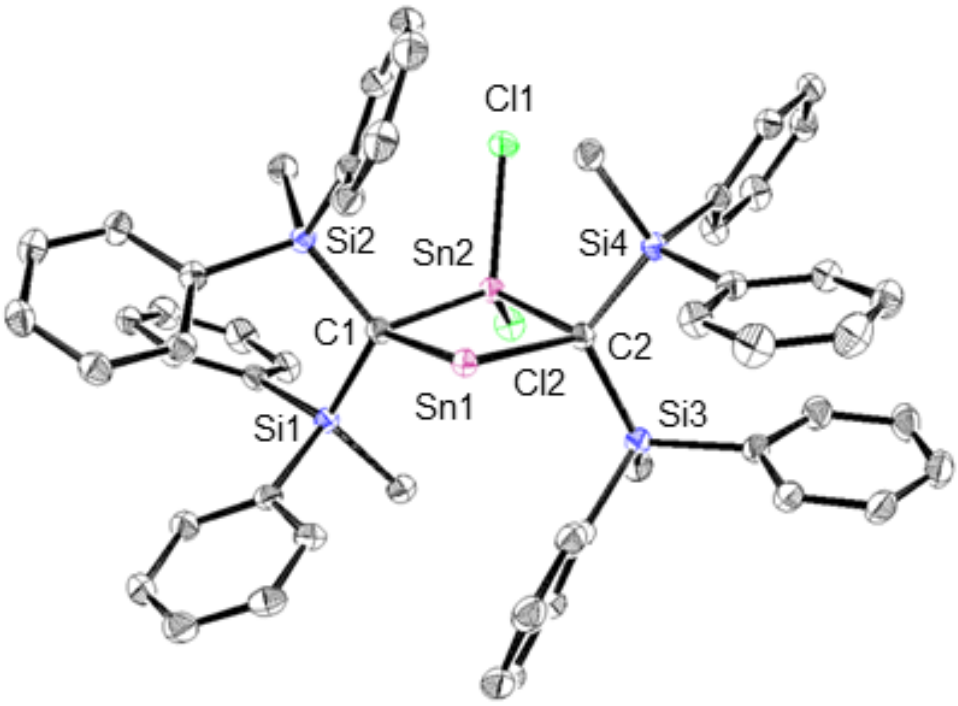

Figure S42. Structure of **5Cl**

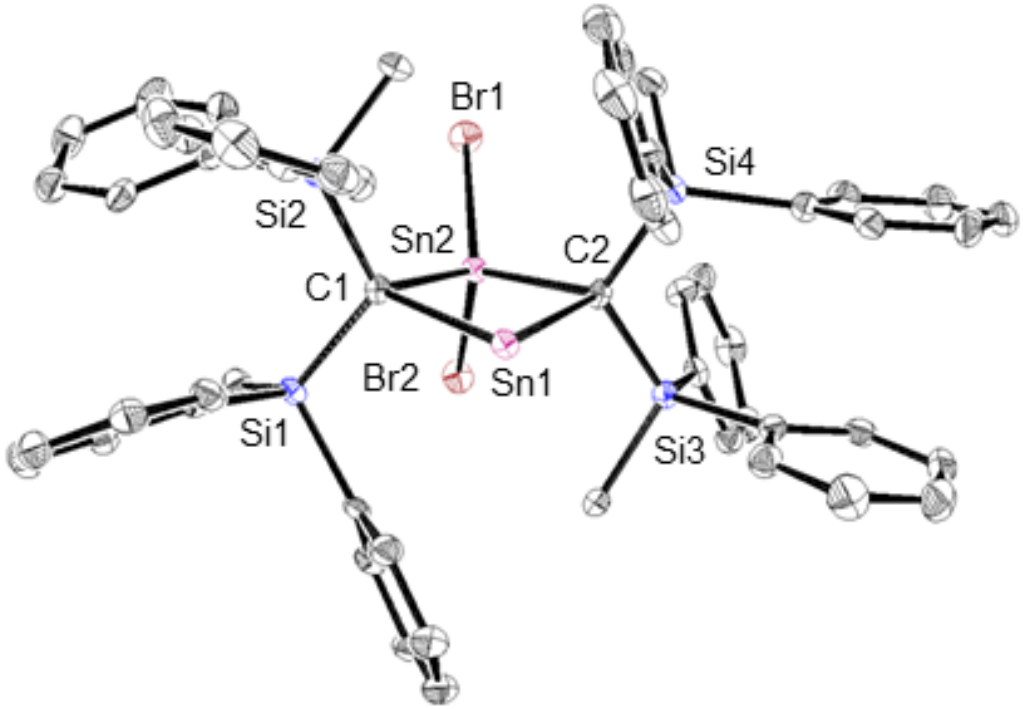

Figure S43. Structure of **5Br**

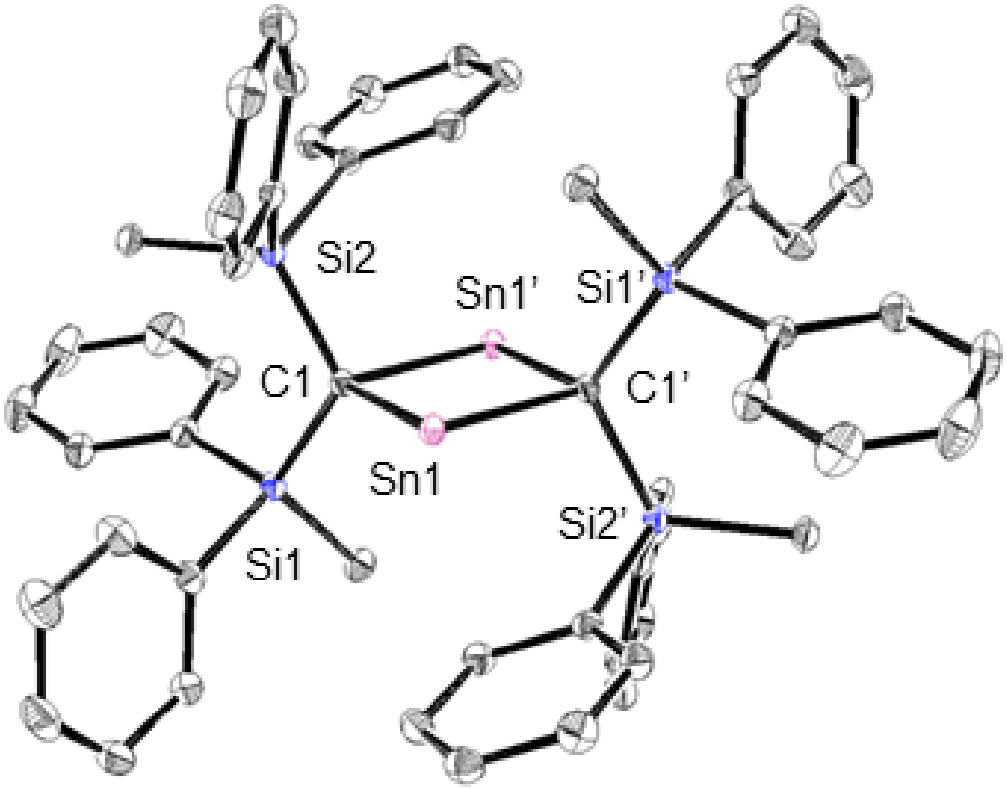

Figure S44. Structure of **6**

Computational Details

All calculations were performed using the Gaussian 16 suite of programs, revision B 01.[S4] The geometry optimization and harmonic vibration frequency calculations of $\mathbf{1_{Sn}}$, $\mathbf{1_{Sn}}$**·THF**, **5Cl**, and **6** were performed using the DFT method at the B3PW91-D3(bj)/Def2TZVP for Sn, 6-311G(2d,p) for the rest atoms level of theory. The frequency calculations confirmed minimum energies for the optimized structures. The optimized geometry of $\mathbf{1_{Sn}}$, $\mathbf{1_{Sn}}$**·THF**, **5Cl**, and **6** are shown in Figure S45, S46, S47 and S48, and selected optimized structural parameters of $\mathbf{1_{Sn}}$, $\mathbf{1_{Sn}}$**·THF**, **5Cl**, and **6** are given in Table S2, Table S3, Table S4, and Table S5. Optimized structures are provided as an xyz file.

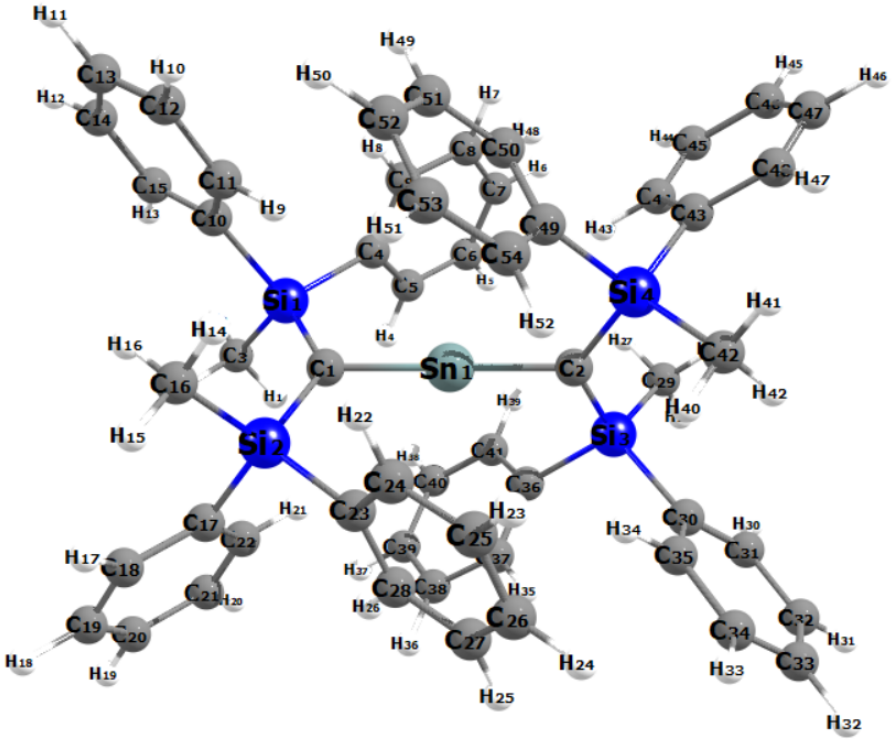

Figure S45. Optimized structure of $\mathbf{1}_{Sn}$.

Table S2. Experimental and calculated values of the bond parameters for compound $\mathbf{1}_{Sn}$.

	Experimental values (Å, deg)	Calculated values (Å, deg)
Sn–C1	1.9787(15)	1.7733
Sn–C2	1.9827(16)	1.7733
C1–Si1	1.8410(16)	1.8655
C1–Si2	1.8336(16)	1.8655
C2–Si3	1.8423(16)	1.8655
C2–Si4	1.8428(16)	1.8655
C1–Sn–C2	178.06(6)	179.98
Sn–C1–Si1	114.62(8)	118.54
Sn–C1–Si2	114.07(8)	118.53
Si1–C1–Si2	130.90(9)	122.93
Sn–C2–Si3	112.17(8)	118.55
Sn–C2–Si4	114.29(8)	118.53
Si3–C2–Si4	133.33(9)	122.93

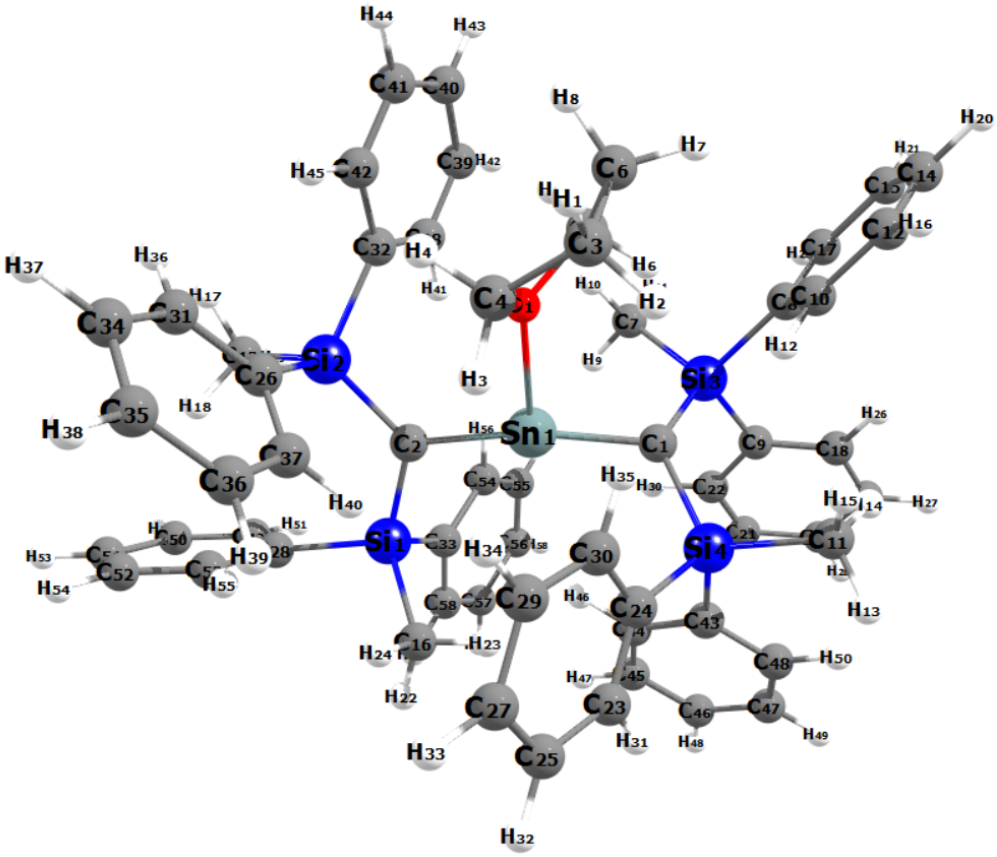

Figure S46. Optimized structure of $\mathbf{1_{Sn}}$·**THF**,

Table S3. Experimental and calculated values of the bond parameters for compound $\mathbf{1_{Sn}}$·**THF**.

		Calculated values (Å, deg)
Sn–C1		1.9741
Sn–C2		1.9722
Sn-O		2.3321
C1–Si1		1.8188
C1–Si2		1.8207
C2–Si3		1.8362
C2–Si4		1.8284
C1–Sn–C2		159.59
Sn–C1–Si1		119.40
Sn–C1–Si2		121.59
Si1–C1–Si2		115.51
Sn–C2–Si3		120.79
Sn–C2–Si4		113.16
Si3–C2–Si4		125.61

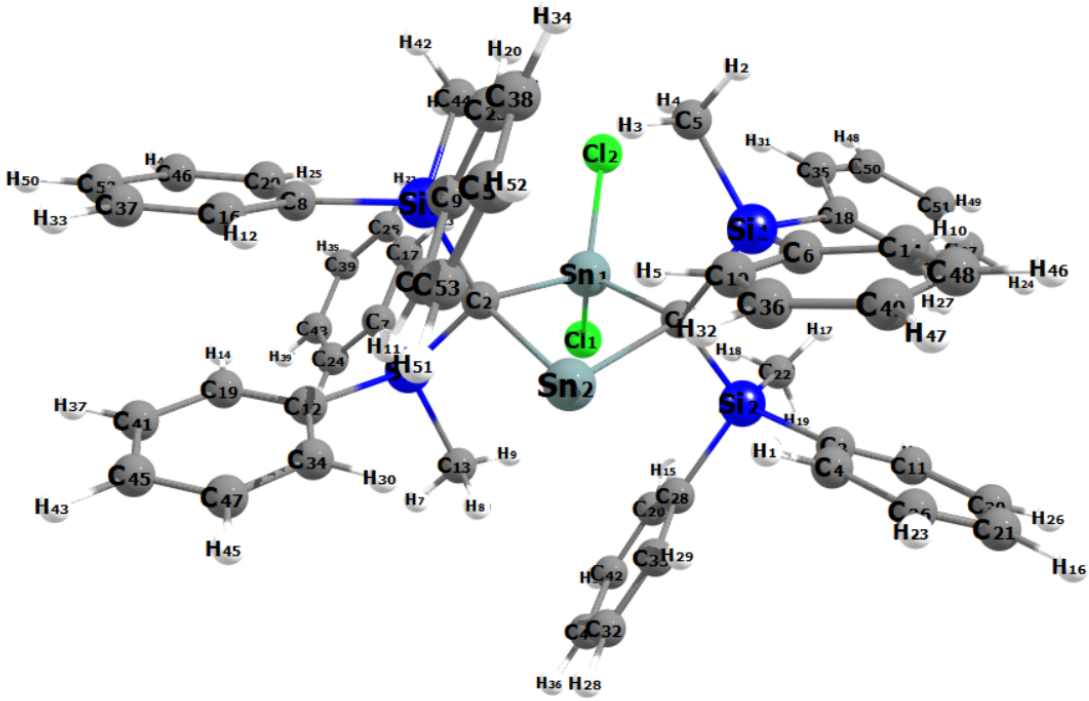

Figure S47. Optimized structure of **5Cl**.

Table S4. Experimental and calculated values of the bond parameters for compound **5Cl**.

	Experimental values (Å, deg)	Calculated values (Å, deg)
Sn1–C1	2.1741(16)	2.1731
Sn1–C2	2.1636(15)	2.1633
C1–Si1	1.8874(16)	1.9017
C1–Si2	1.9051(16)	1.9092
Sn1-Cl1	2.3690(4)	2.3689
Sn1-Cl2	2.3708(4)	2.3721
Sn2-C1	2.2996(15)	2.3005
Sn2-C2	2.3119(15)	2.3132
C2–Si3	1.9017(16)	1.8876
C2–Si4	1.9095(16)	1.9047
C1–Sn1–C2	87.97(5)	87.926
C1–Sn2–C2	95.17(6)	95.224
Sn1-C1-Sn2	87.69(5)	87.667
Sn1-C2-Sn2	87.75(6)	87.758

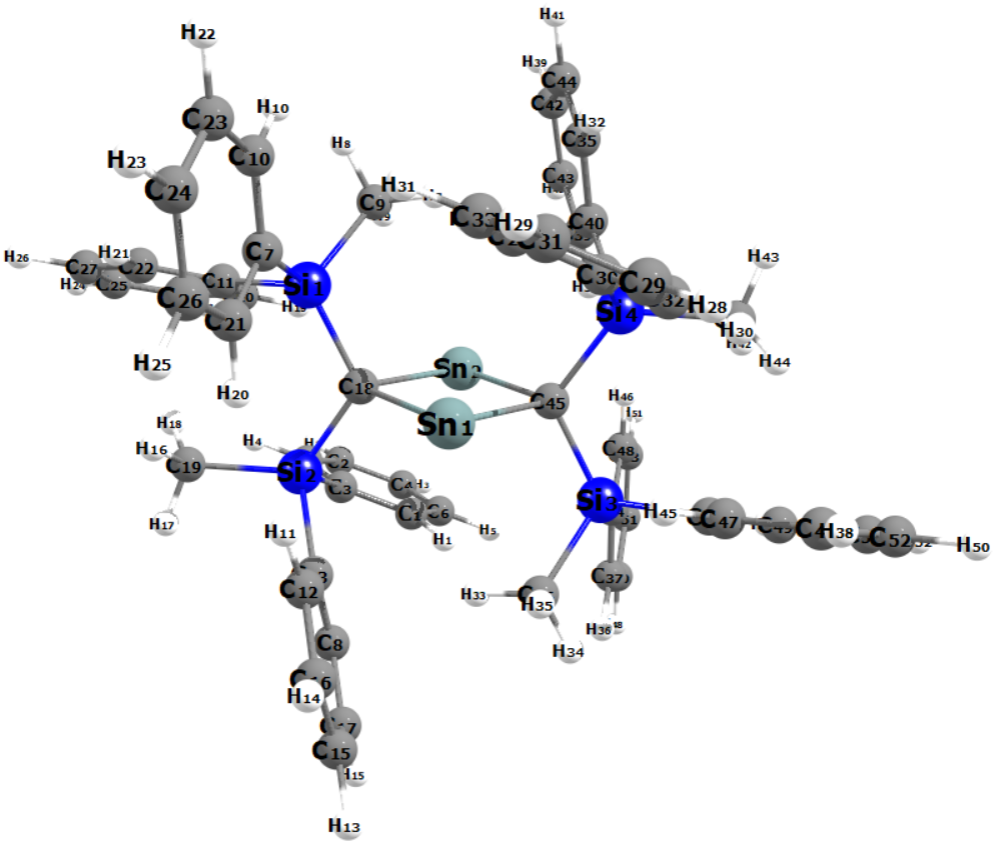

Figure S48. Optimized structure of **6**.

Table S5. Experimental and calculated values of the bond parameters for compound **6**.

	Experimental values (Å, deg)	Calculated values (Å, deg)
Sn1–C18	2.301(1)	2.2992
Sn1–C45	2.281(2)	2.1633
C18–Si1	1.862(1)	1.8493
C18–Si2	1.871(1)	1.8609
Sn2-C18	2.301(1)	2.3395
Sn2-C45	2.281(2)	2.2991
C45–Si3	1.862(1)	1.8493
C45–Si4	1.871(1)	1.8609
C18–Sn1–C45	87.47(4)	84.777
C18–Sn2–C45	87.47(4)	84.780
Sn1-C18-Sn2	92.58(4)	95.221
Sn1-C45-Sn2	92.58(4)	95.222

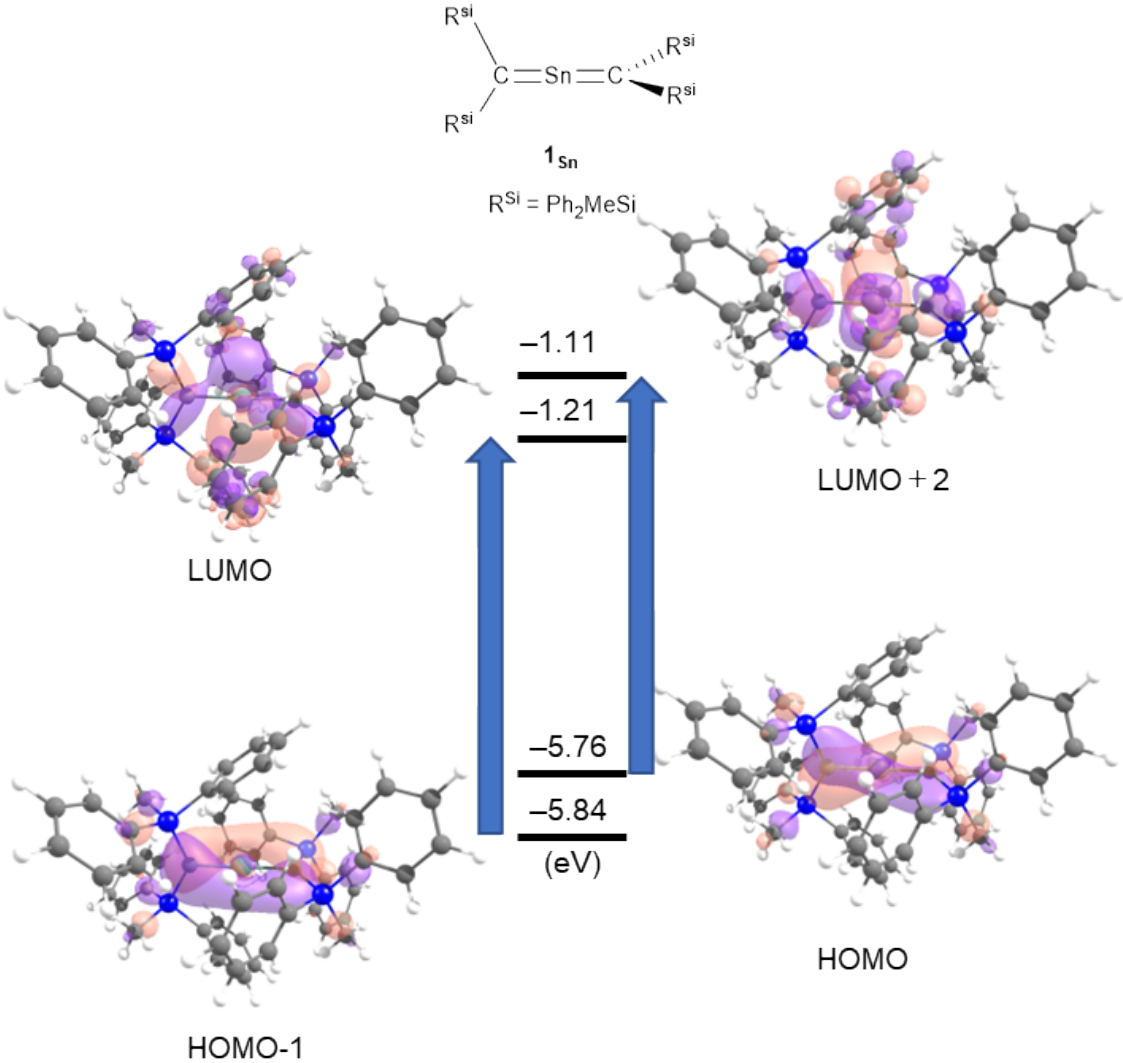

Figure S49. Kohn-Sham molecular orbitals of 2-stannapropadiene [B3PW91-D3(bj)/Def2TZVP for Sn, 6-311G(2d,p) for the rest atoms, together with the chemical structure. The HOMO and HOMO-1 involve the two C-Sn π-bonds. The LUMO and LUMO+2 involve the two C-Sn π*-bonds.

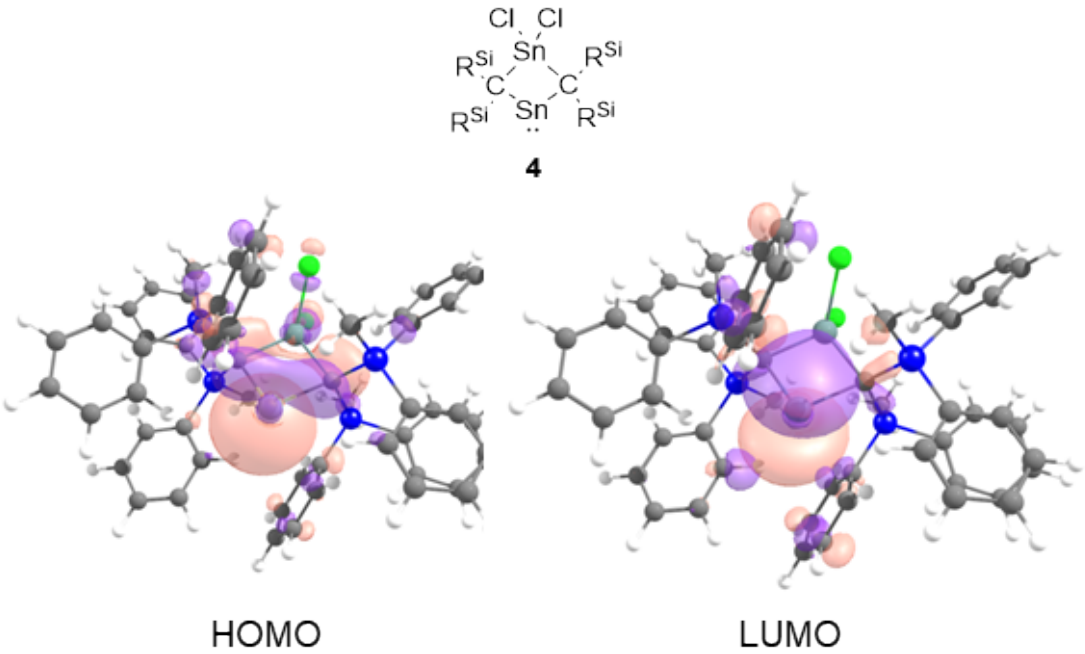

Figure S50. Kohn-Sham molecular orbitals of stannylene **5Cl** [B3PW91-D3(bj)/Def2TZVP for Sn, 6-311G(2d,p) for the rest atoms, together with the chemical structure. The HOMO involves the lone pair of Sn atom and the LUMO involves the vacant p-orbitals of Sn atom.

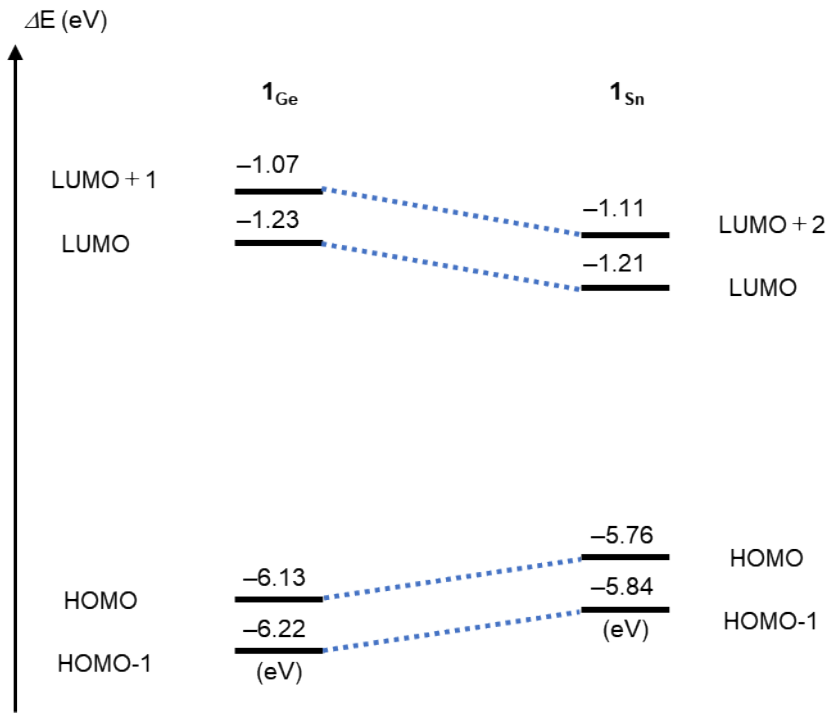

Figure S51. Presentation of the energy levels of $\mathbf{1}_{Sn}$ and $\mathbf{1}_{Ge}$.

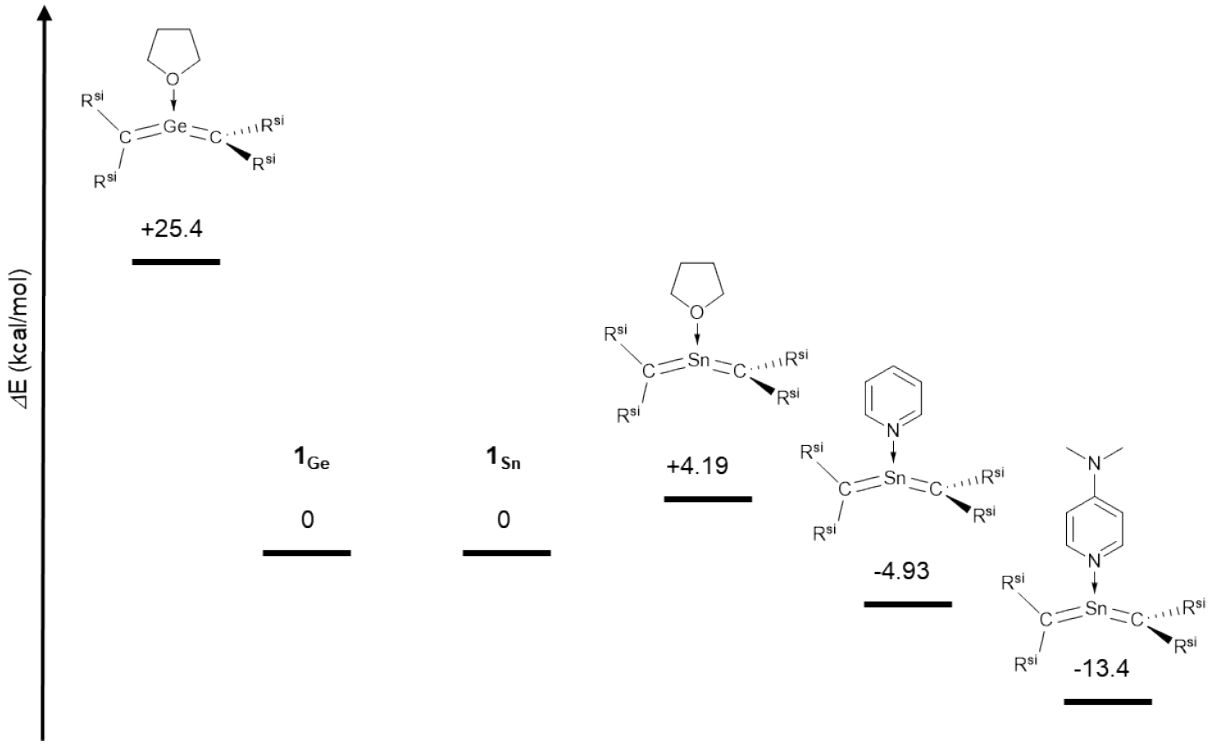

Figure S52. Relative energies of the 2-heterapropadienes and their donor coordinated compounds.

Infrared Spectroscopy

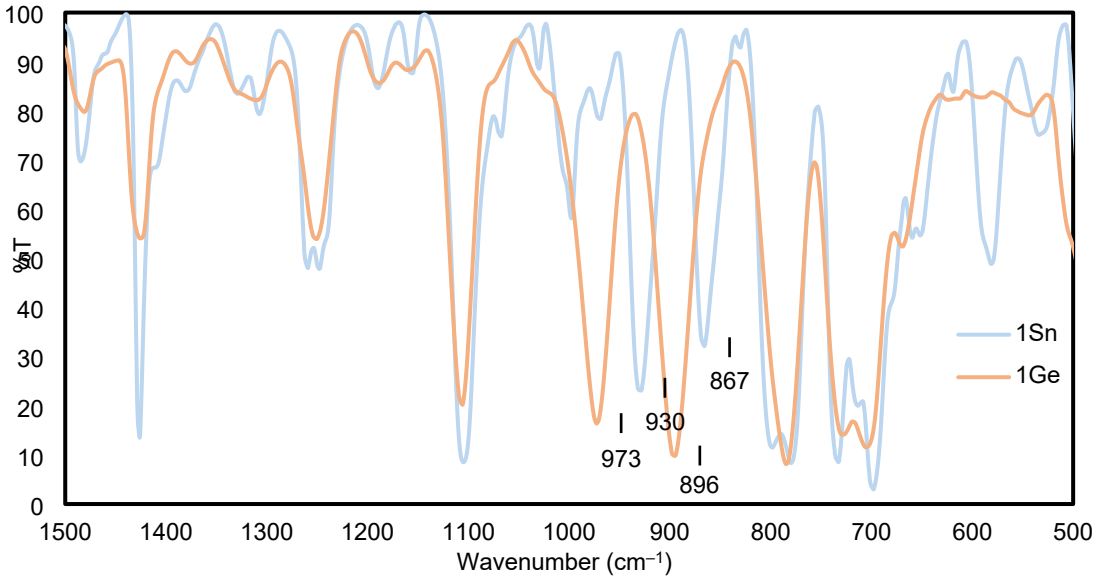

Figure S53. Infrared Spectra of $\mathbf{1}_{Ge}$ and $\mathbf{1}_{Sn}$.

UV-vis Spectroscopy

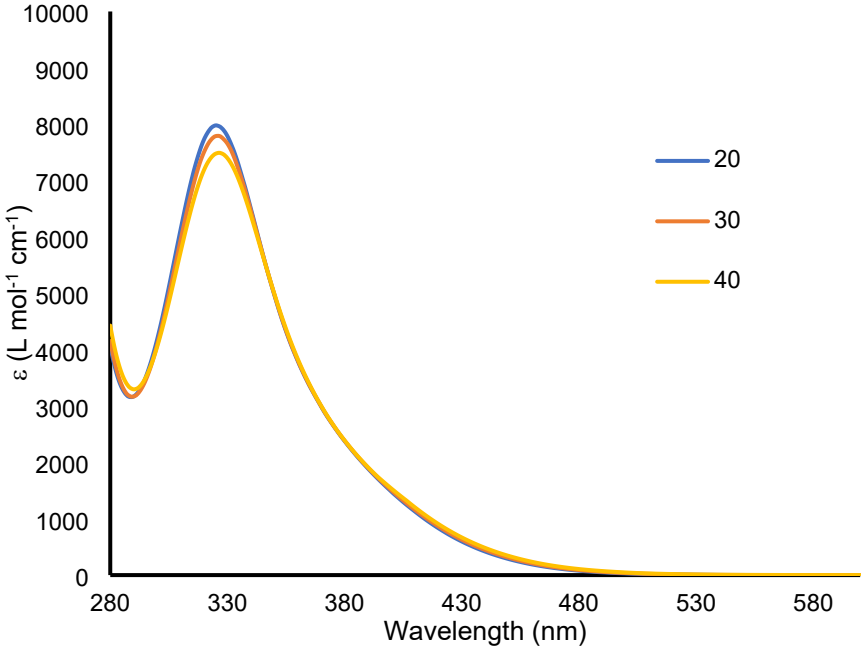

Figure S54. Variable temperature UV-vis Spectra of $\mathbf{1_{Sn}}$ in benzene (1.6×10^{-3} M) at 20, 30, and 40 °C.

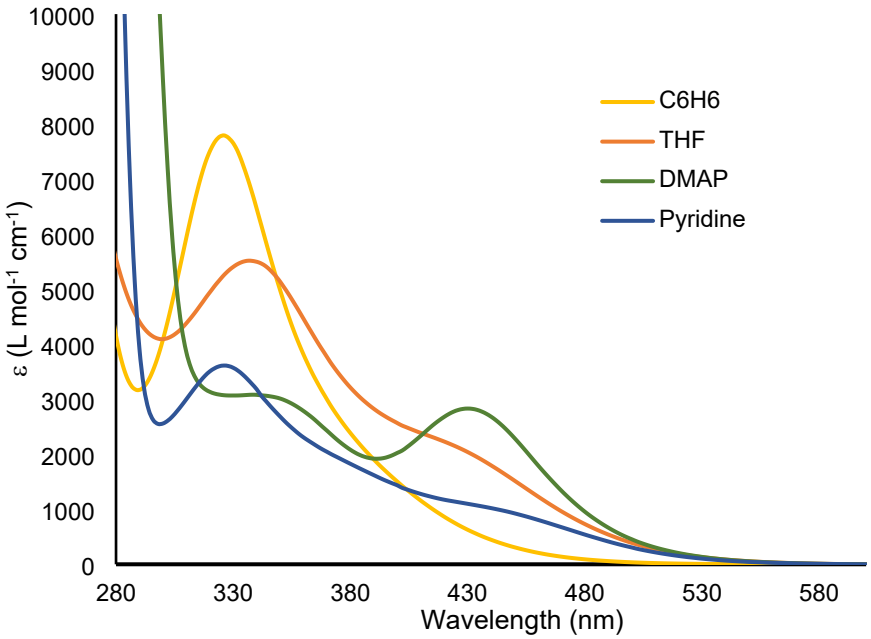

Figure S55. UV-vis Spectra of $\mathbf{1_{Sn}}$ in benzene (1.6×10^{-3} M), in THF (1.6×10^{-3} M), $\mathbf{1_{Sn}}$**·Pyridine** (1.6×10^{-3} M of $\mathbf{1_{Sn}}$ with equimolar of pyridine), and $\mathbf{1_{Sn}}$**·DMAP** (1.6×10^{-3} M of $\mathbf{1_{Sn}}$ with equimolar of DMAP)**.**

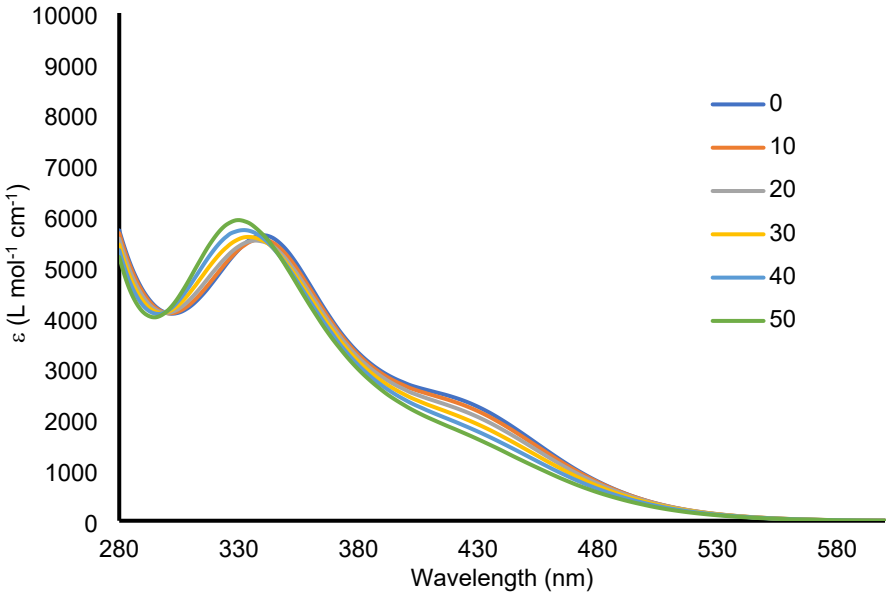

Figure S56. Variable temperature UV-vis Spectra of $\mathbf{1_{Sn}}$ in THF (1.6×10^{-3} M) at 0-50 °C.

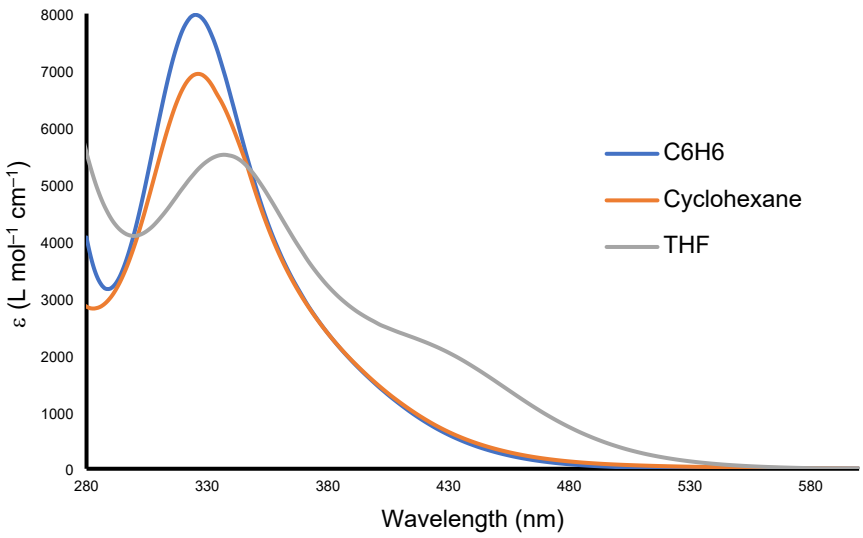

Figure S57. UV-vis Spectra of $\mathbf{1_{Sn}}$ in C_6H_6 (1.6×10^{-3} M), Cyclohexane (0.8×10^{-3} M), THF (1.6×10^{-3} M) at 20 °C.

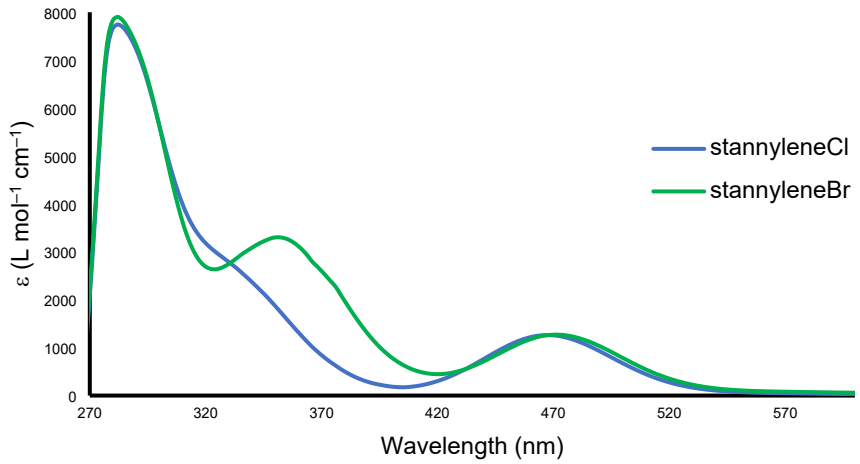

Figure S58. UV-vis Spectra of **5Cl** and **5Br** in benzene (1.5×10^{-3} M) at room temperature.

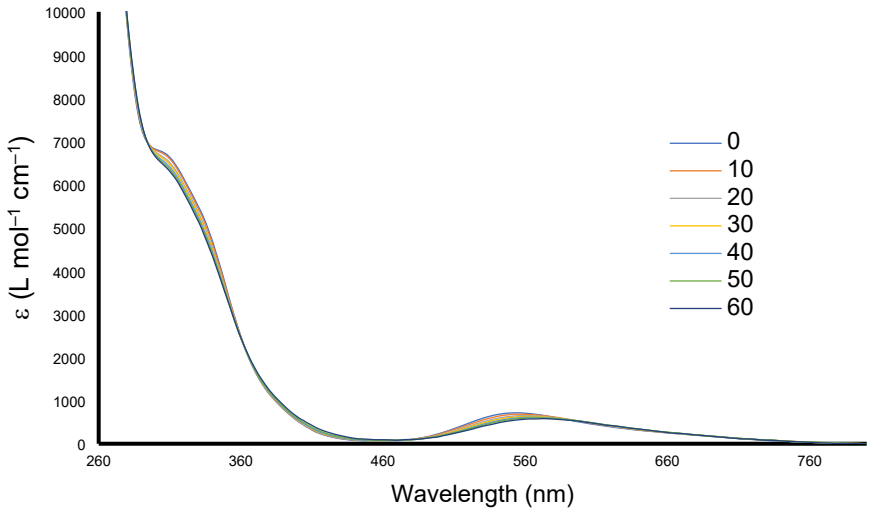

Figure S59. Variable temperature UV-vis Spectra of **6** in THF (1.6×10^{-3} M) at 0-60 ℃.

[S1] G. M. Sheldrick, Acta Cryst., 2015, A71, 3-8.

[S2] G. M. Sheldrick, Acta Cryst., 2015, C71, 3-8.

[S3] Wakita, K. (2001). Yadokari-XG. Software for Crystal Structure Analyses. Release of Software (Yadokari-XG 2009) for Crystal Structure Analyses, Kabuto, C., Akine, S., Nemoto, T. and Kwon, E. (2009). J. Cryst. Soc. Jpn., 51, 218-224.

[S4] Gaussian 16, Revision B.01, Frisch, M. J.; Trucks, G. W.; Schlegel, H. B.; Scuseria, G. E.; Robb, M. A.; Cheeseman, J. R.; Scalmani, G.; Barone, V.; Petersson, G. A.; Nakatsuji, H.; Li, X.; Caricato, M.; Marenich, A. V.; Bloino, J.; Janesko, B. G.; Gomperts, R.; Mennucci, B.; Hratchian, H. P.; Ortiz, J. V.; Izmaylov, A. F.; Sonnenberg, J. L.; Williams-Young, D.; Ding, F.; Lipparini, F.; Egidi, F.; Goings, J.; Peng, B.; Petrone, A.; Henderson, T.; Ranasinghe, D.; Zakrzewski, V. G.; Gao, J.; Rega, N.; Zheng, G.; Liang, W.; Hada, M.; Ehara, M.; Toyota, K.; Fukuda, R.; Hasegawa, J.; Ishida, M.; Nakajima, T.; Honda, Y.; Kitao, O.; Nakai, H.; Vreven, T.; Throssell, K.; Montgomery, Jr., J. A.; Peralta, J. E.; Ogliaro, F.; Bearpark, M. J.; Heyd, J. J.; Brothers, E. N.; Kudin, K. N.; Staroverov, V. N.; Keith, T. A.; Kobayashi, R.; Normand, J.; Raghavachari, K.; Rendell, A. P.; Burant, J. C.; Iyengar, S. S.; Tomasi, J.; Cossi, M.; Millam, J. M.; Klene, M.; Adamo, C.; Cammi, R.; Ochterski, J. W.; Martin, R. L.; Morokuma, K.; Farkas, O.; Foresman, J. B.; Fox, D. J. Gaussian, Inc., Wallingford CT, 2016.